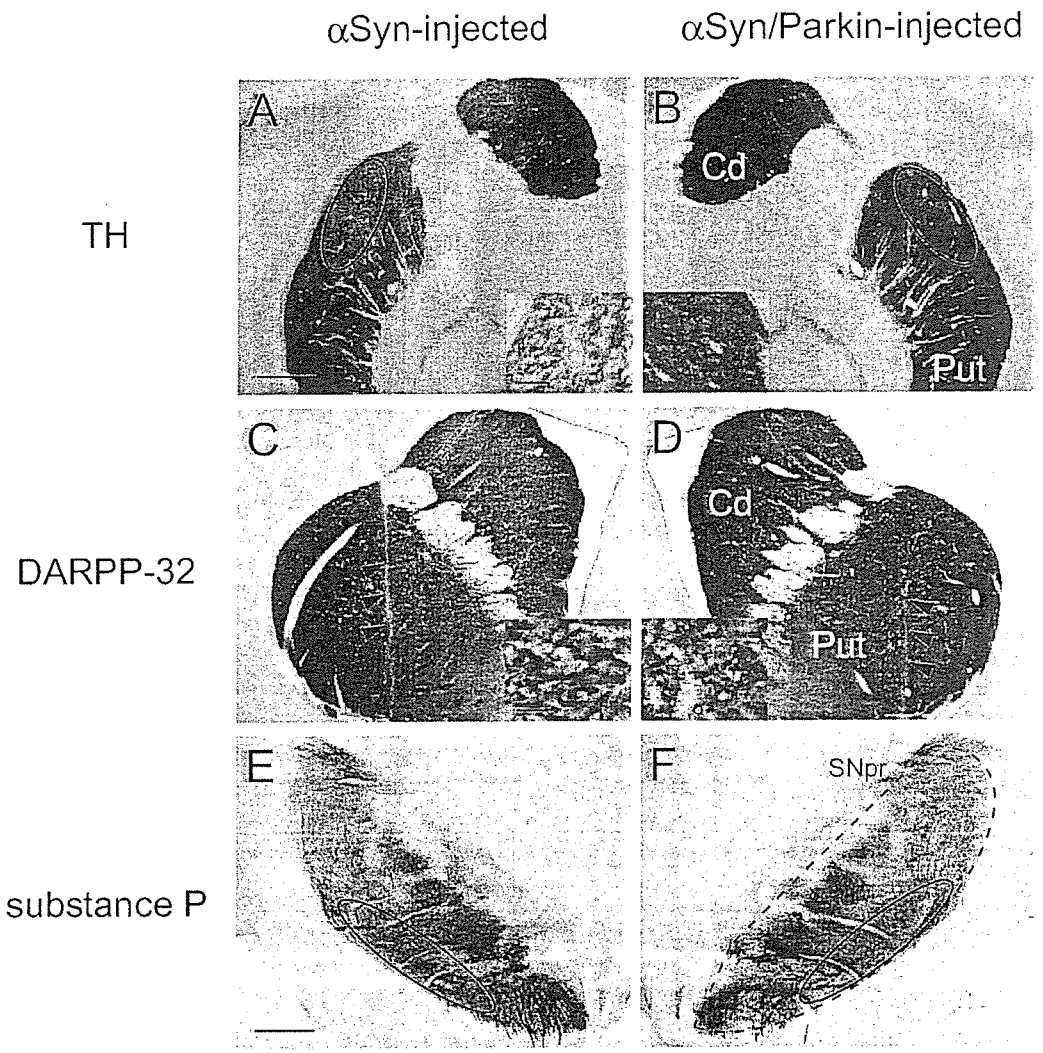

Fig. 4. Immunostaining of dopaminergic and GABAergic neurons. Photographs of the side injected with rAAV1-αSyn alone (A, C, and E; αSyn-injected) and the side injected with a cocktail of rAAV1-αSyn and rAAV1-parkin (B, D, and F; αSyn/Parkin-injected) are represented. (A, B, and inset: enlarged images) Immunoreactivity for TH in the putamen. Note the weaker immunoreactivity for TH on the side injected with rAAV1-αSyn alone (A), compared with the other side injected with a cocktail of rAAV1-αSyn and rAAV1-parkin (B). The dorsolateral portion of the putamen (Put) subjected to densitometric quantification is shown by open ellipse (A and B). (C–F) Immunoreactivities for DARPP-32 in the putamen (C, D, and inset: enlarged images) and for substance P in the SNpr (E, F). There is no apparent decrease in DARPP-32- or substance P-immunoreactivity. The track of the injection needle around which the DARPP-32-positive cells are counted is shown by closed arrowheads (C and D). The ventrolateral portion of the SNpr subjected to densitometric quantification is shown by open ellipse (E and F). Scale bar=2-mm in A (A–D); in A inset, 100-μm (A, B inset); in C inset, 50-μm (C, D inset); and in E, 1-mm (E, F). Caudate (Cd) and Put areas are indicated in B and D; and the SNpr is circumscribed by dotted line in F.

with the side co-injected with rAAV1-parkin. This might be ascribed to the αSyn-induced dopaminergic neurodegeneration and the possible protection against it by virally introduced Parkin activity. In favor of such a conclusion, almost no dopaminergic cells in the SNpc displayed αSyn immunoreactivity, whereas a number of single SNpc cells were immunoreactive for both αSyn and Parkin. When the number of TH-positive cells was counted in the SNpc, we could not find a significant difference between the sides injected with rAAV1-αSyn alone and a cocktail of rAAV1-αSyn and rAAV1-parkin. This may be attributed to insufficient retrograde transport of delivered genes. In fact, we found that 25–30 cells in the SNpc were double-labeled with αSyn/Parkin per section on the side injected with a cocktail of rAAV1-αSyn and rAAV1-parkin. Even if a similar number of dopaminergic cells could be transduced with rAAV1-αSyn on the opposite side to degenerate definitively, loss of such a small number of dopaminergic cells might not lead to a statistically significant difference between the two sides. In the other monkey, no explicit change in striatal TH immunoreactivity was detected. In this monkey, only a few single neurons in the SNpc contained both αSyn and Parkin proteins. However, we observed a comparable level of αSyn and Parkin expression

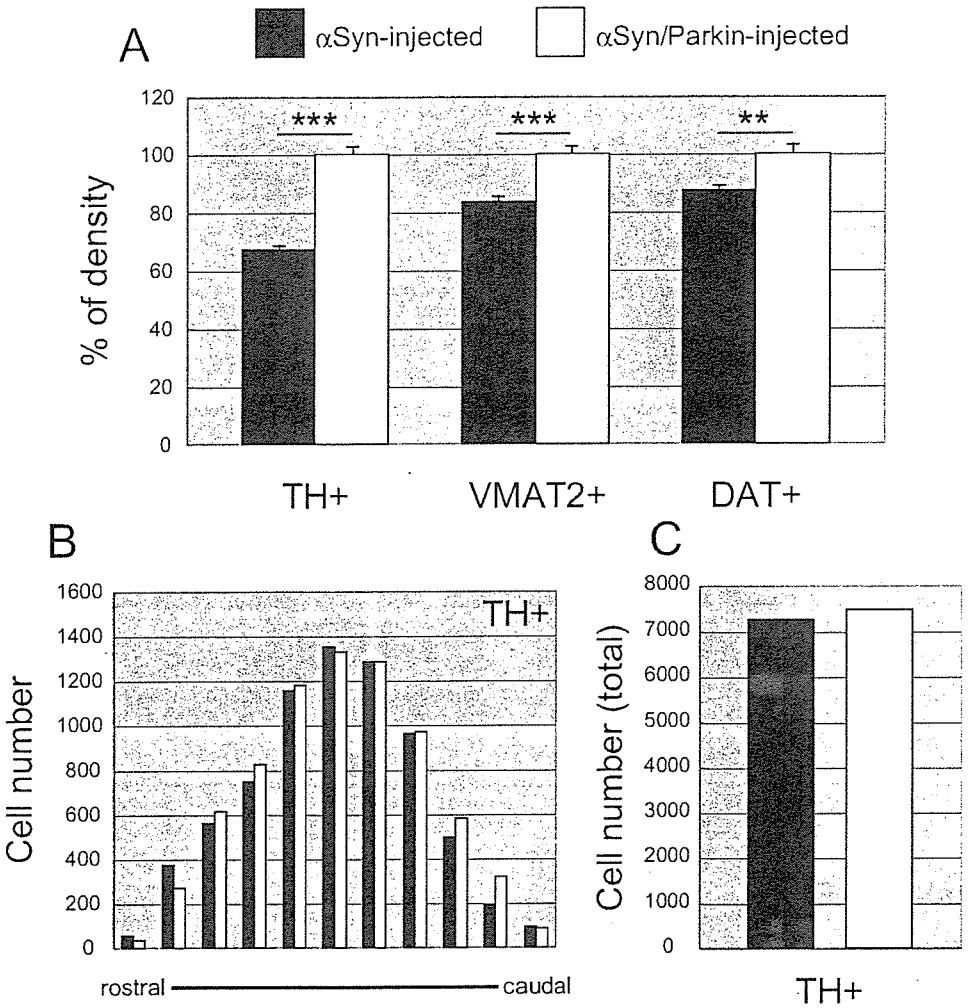

Fig. 5. Effects of protein expression on dopaminergic neurons. (A–C) The filled box indicates the data on the side injected with rAAV1-αSyn alone, and the open box indicates the data on side injected with a cocktail of rAAV1-αSyn and rAAV1-parkin. (A) The density of dopaminergic axon terminals immunostained for TH (indicated by TH+), VMAT2 (VMAT2+), or DAT (DAT+). The data are expressed as % to the data on the side injected with a cocktail of rAAV1-αSyn and rAAV1-parkin. Note the significant decrease in dopaminergic axon terminals on the side injected with rAAV1-αSyn alone. (B, C) The number of TH-positive (TH+) cell numbers in every tenth coronal section in the SNpc (B) and in the entire SNpc (C). The cell number had no difference between the two sides. ** $P<0.01$, *** $P<0.001$.

in GABAergic neurons to that in the monkey killed at the 4-month post-injection period, suggesting that the faint effect on dopaminergic neurons may not be due to a progressive down-regulation of delivered gene expression. Daadi et al. (2006) have recently reported that rAAV-mediated gene expression lasted at least 3 years. Therefore, the absence of neurodegenerative signs may be attributable to a relatively insufficient delivery of rAAV1 vectors to dopaminergic axon terminals in the monkey killed at the 7.5-month post-injection period.

On the other hand, no apparent degeneration of striatal GABAergic neurons was observed, although accumulation of Ser129-phosphorylated αSyn protein was noted. These results imply the selective dopaminergic toxicity of Ser129-phosphorylated αSyn protein. Recently, it has been reported that phosphorylation at Ser129 residue is essential for αSyn to induce some neuronal toxicity in a *Drosophila* model of PD (Chen and Feany, 2005). The αSyn toxicity is abolished by amino acid substitution Ser129Ala which is no longer phosphorylated, and is reproduced by Ser129Asp which carries a negative charge mimicking phosphate on serine residue. However, Ser129-phosphorylation occurs immediately after expression of *αSyn* transgene (Chen and Feany, 2005), which is observed considerably earlier than the apparent neurodegeneration in the fly nervous system. Another event, e.g. oxidative modification by reactive oxygen species generated in dopamine metabolism, may therefore be indispensable for the Ser129-phosphorylated αSyn protein to gain a neurotoxic property. Several important findings can explain the selective vulnerability of dopaminergic neurons in PD development: dopaminergic toxicity of αSyn protein (Xu et al., 2002), age-dependent stabilization of αSyn protein in the SNpc (Li et al., 2004), and change in aggregation propen-

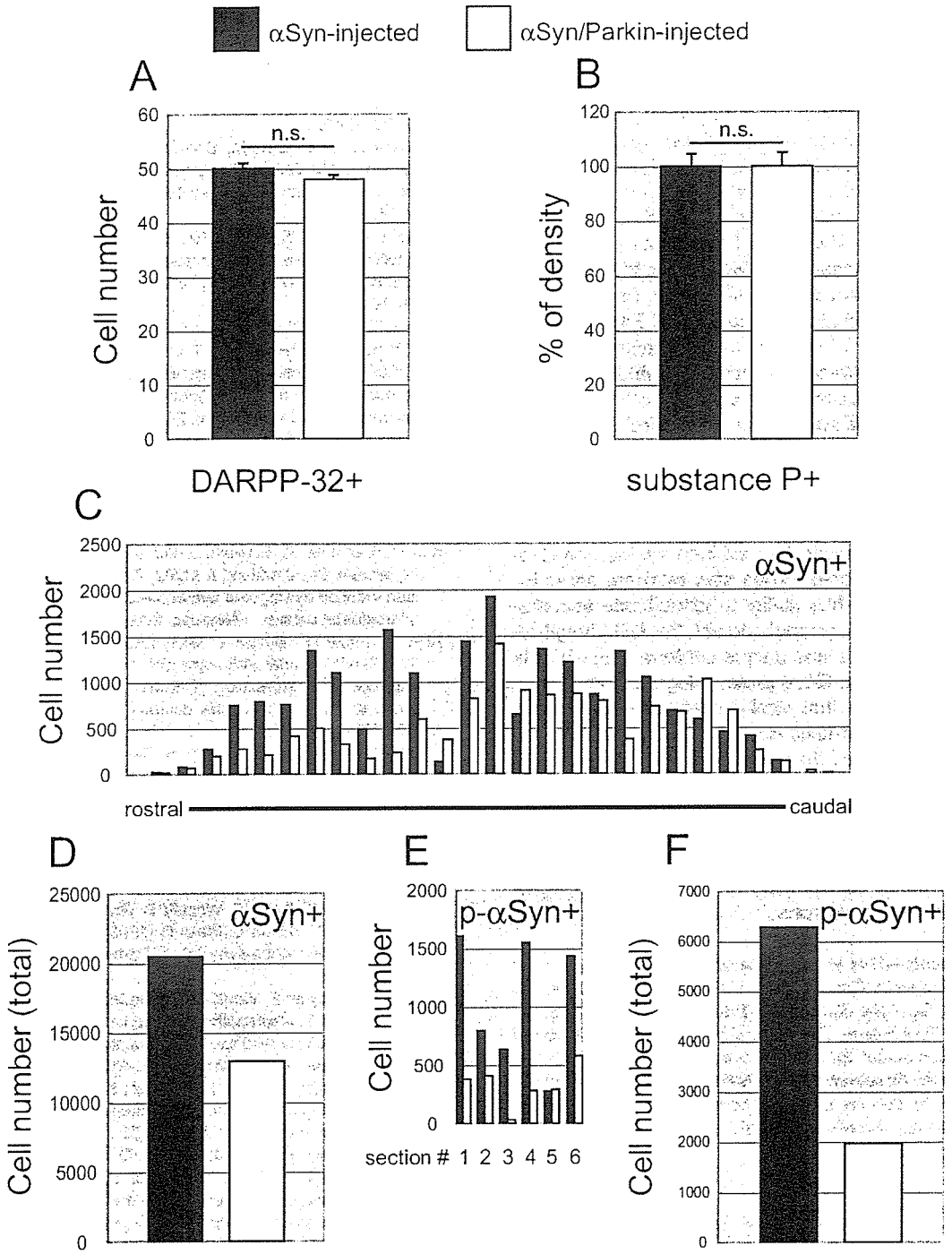

Fig. 6. Effects of protein expression on GABAergic neurons. (A–F) The filled box indicates the data on the side injected with rAAV1-αSyn alone, and the open box indicates the data on side injected with a cocktail of rAAV1-αSyn and rAAV1-parkin. (A, B) The number of DARPP-32-positive (indicated by DARPP-32+) cell bodies in the putamen (A) and the density of substance P-positive (substance P+) axon terminals in the SNpr (B). There is no significant change in striatonigral GABAergic neurons on both sides. (C, D) The number of the αSyn-positive (αSyn+) cell numbers in every tenth coronal section (C) and in the entire putamen (D). (E, F) The number of the Ser129-phosphorylated αSyn (p-αSyn)-positive (p-αSyn+) cell numbers in every sixth section from medial part of the putamen (E) and the total number of them (F). There is apparent decrease in the numbers of the αSyn+ and p-αSyn+ cells on the side injected with a cocktail of rAAV1-αSyn and rAAV1-parkin. n.s., not significant.

sity of αSyn by covalent modification by dopamine (Conway et al., 2001). **A similar oxidative modification has recently been shown for Parkin proteins: *S*-nitrosylation (Chung et al., 2004; Yao et al., 2004) or covalent binding of dopamine (LaVoie et al., 2005) results in the impairment of E3 ubiquitin ligase activity, which may be responsible for**

the development of sporadic PD. Endogenous Parkin in healthy SNpc dopaminergic neurons could be subjected to this modification, thereby lowering the threshold for the onset of neurodegenerative molecular cascades triggered by the accumulated Ser129-phosphorylated αSyn protein.

The accumulation and/or Ser129-phosphorylation of αSyn in GABAergic neurons were reduced on the Parkin-delivered side. Previous reports showed a successful transduction of three different genes to single neurons using a cocktail of rAAV vectors (Shen et al., 2000; Muramatsu et al., 2002). Accordingly, we believe that the lower accumulation/phosphorylation of αSyn may be caused by protein clearance promoted by transduced Parkin but not by virus interference. We found similar extents of the distribution areas of αSyn-positive neurons within the putamen on both sides (Fig. 6C). This implies that the resultant increase in the volume and dilution of the viral suspension on the side injected with a cocktail of rAAV1-αSyn and rAAV1-parkin had a negligible effect. The rationale for a decrease in αSyn accumulation in response to Parkin delivery could be speculated as follows; 1) a protein stabilizing αSyn may be removed by Parkin-mediated polyubiquitination, 2) the delivered Parkin may extricate some E3 ubiquitin ligase which has ability to ubiquitinate accumulated αSyn, and 3) the accumulated and Ser129-phosphorylated αSyn may form some unique conformation which is subjected to Parkin-mediated protein degradation.

Our data indicate that virally overexpressed Parkin protein ablates the non-toxic αSyn protein accumulated in GABAergic neurons and the toxic species in dopaminergic neurons. Accordingly, parkin gene therapy may be potentially effective in the treatment of sporadic PD. Further studies are needed to examine possible negative effect of Parkin overexpression on healthy neurons, and to refine the rAAV-mediated transduction of parkin gene to nigrostriatal dopaminergic neurons.

Acknowledgments—This work was supported in part by a High Technology Research Center grant, a Grant-in-Aid for Scientific Research (B) from the Ministry of Education, Culture, Sports, Science, and Technology, Japan, and a grant from the National Institute of Biomedical Innovation. We are grateful to staff in Tsukuba Primate Research Center, National Institute of Biomedical Innovation, for their handling and care of the monkeys. We are also grateful to Ms. Michiko Imanishi for her excellent technical assistance.

REFERENCES

Chen L, Feany MB (2005) Alpha-synuclein phosphorylation controls neurotoxicity and inclusion formation in a Drosophila model of Parkinson disease. Nat Neurosci 8:657–663.

Chung KK, Thomas B, Li X, Pletnikova O, Troncoso JC, Marsh L, Dawson VL, Dawson TM (2004) *S*-nitrosylation of parkin regulates ubiquitination and compromises parkin's protective function. Science 304:1328–1331.

Conway KA, Rochet JC, Bieganski RM, Lansbury PT Jr (2001) Kinetic stabilization of the alpha-synuclein protofibril by a dopamine-alpha-synuclein adduct. Science 294:1346–1349.

Daadi MM, Pivirotto P, Bringas J, Cunningham J, Forsayeth J, Eberling J, Bankiewicz KS (2006) Distribution of AAV2-hAADC-transduced cells after 3 years in Parkinsonian monkeys. Neuroreport 17:201–204.

da Costa CA, Ancolio K, Checler F (2000) Wild-type but not Parkinson's disease-related Ala-53>Thr mutant alpha-synuclein protects neuronal cells from apoptotic stimuli. J Biol Chem 275: 24065–24069.

Fujiwara H, Hasegawa M, Dohmae N, Kawashima A, Masliah E, Goldberg MS, Shen J, Takio K, Iwatsubo T (2002) Alpha-synuclein is phosphorylated in synucleinopathy lesions. Nat Cell Biol 4:160–164.

Giasson BI, Duda JE, Quinn SM, Zhang B, Trojanowski JQ, Lee VM (2002) Neuronal alpha-synucleinopathy with severe movement disorder in mice expressing A53T human alpha-synuclein. Neuron 34:521–533.

Gispert S, Del Turco D, Garrett L, Chen A, Bernard DJ, Hamm-Clement J, Korf HW, Deller T, Braak H, Auburger G, Nussbaum RL (2003) Transgenic mice expressing mutant A53T human alpha-synuclein show neuronal dysfunction in the absence of aggregate formation. Mol Cell Neurosci 24:419–429.

Goedert M (2001) Alpha-synuclein and neurodegenerative diseases. Nat Rev Neurosci 2:492–501.

Hashimoto M, Rockenstein E, Masliah E (2003) Transgenic models of alpha-synuclein pathology: past, present, and future. Ann N Y Acad Sci 991:171–188.

Kirik D, Rosenblad C, Burger C, Lundberg C, Johansen TE, Muzyczka N, Mandel RJ, Bjorklund A (2002) Parkinson-like neurodegeneration induced by targeted overexpression of alpha-synuclein in the nigrostriatal system. J Neurosci 22:2780–2791.

Kirik D, Annett LE, Burger C, Muzyczka N, Mandel RJ, Bjorklund A (2003) Nigrostriatal alpha-synucleinopathy induced by viral vector-mediated overexpression of human alpha-synuclein: a new primate model of Parkinson's disease. Proc Natl Acad Sci U S A 100:2884–2889.

Kitada T, Asakawa S, Hattori N, Matsumine H, Yamamura Y, Minoshima S, Yokochi M, Mizuno Y, Shimizu N (1998) Mutations in the parkin gene cause autosomal recessive juvenile parkinsonism. Nature 392:605–608.

Klein RL, King MA, Hamby ME, Meyer EM (2002) Dopaminergic cell loss induced by human A30P alpha-synuclein gene transfer to the rat substantia nigra. Hum Gene Ther 13:605–612.

Kruger R, Kuhn W, Muller T, Woitalla D, Graeber M, Kosel S, Przuntek H, Epplen JT, Schols L, Riess O (1998) Ala30Pro mutation in the gene encoding alpha-synuclein in Parkinson's disease. Nat Genet 18:106–108.

Lauwers E, Debyser Z, Van Dorpe J, De Strooper B, Nuttin B, Baekelandt V (2003) Neuropathology and neurodegeneration in rodent brain induced by lentiviral vector-mediated overexpression of alpha-synuclein. Brain Pathol 13:364–372.

LaVoie MJ, Ostaszewski BL, Weihofen A, Schlossmacher MG, Selkoe DJ (2005) Dopamine covalently modifies and functionally inactivates parkin. Nat Med 11:1214–1221.

Lee MK, Stirling W, Xu Y, Xu X, Qui D, Mandir AS, Dawson TM, Copeland NG, Jenkins NA, Price DL (2002) Human alpha-synuclein-harbouring familial Parkinson's disease-linked Ala-53>Thr mutation causes neurodegenerative disease with alpha-synuclein aggregation in transgenic mice. Proc Natl Acad Sci U S A 99:8968–8973.

Li W, Lesuisse C, Xu Y, Troncoso JC, Price DL, Lee MK (2004) Stabilization of alpha-synuclein protein with aging and familial Parkinson's disease-linked A53T mutation. J Neurosci 24:7400–7409.

Lo Bianco C, Ridet JL, Schneider BL, Deglon N, Aebischer P (2002) Alpha-synucleinopathy and selective dopaminergic neuron loss in a rat lentiviral-based model of Parkinson's disease. Proc Natl Acad Sci U S A 99:10813–10818.

Lo Bianco C, Schneider BL, Bauer M, Sajadi A, Brice A, Iwatsubo T, Aebischer P (2004) Lentiviral vector delivery of parkin prevents dopaminergic degeneration in an alpha-synuclein rat model of Parkinson's disease. Proc Natl Acad Sci U S A 101:17510–17515.

Martin LJ, Pan Y, Price AC, Sterling W, Copeland NG, Jenkins NA, Price DL, Lee MK (2006) Parkinson's disease alpha-synuclein transgenic mice develop neuronal mitochondrial degeneration and cell death. J Neurosci 26:41–50.

Masliah E, Rockenstein E, Veinbergs I, Mallory M, Hashimoto M, Takeda A, Sagara Y, Sisk A, Mucke L (2000) Dopaminergic loss and inclusion body formation in alpha-synuclein mice: implications for neurodegenerative disorders. Science 287:1265–1269.

Matsuoka Y, Vila M, Lincoln S, McCormack A, Picciano M, LaFrancois J, Yu X, Dickson D, Langston WJ, McGowan E, Farrer M, Hardy J, Duff K, Przedborski S, Di Monte DA (2001) Lack of nigral pathology in transgenic mice expressing human alpha-synuclein driven by the tyrosine hydroxylase promoter. Neurobiol Dis 8:535–539.

Muramatsu S, Fujimoto K, Ikeguchi K, Shizuma N, Kawasaki K, Ono F, Shen Y, Wang L, Mizukami H, Kume A, Matsumura M, Nagatsu I, Urano F, Ichinose H, Nagatsu T, Terao K, Nakano I, Ozawa K (2002) Behavioral recovery in a primate model of Parkinson's disease by triple transduction of striatal cells with adeno-associated viral vectors expressing dopamine-synthesizing enzymes. Hum Gene Ther 13:345–354.

Neumann M, Kahle PJ, Giasson BI, Ozmen L, Borroni E, Spooren W, Muller V, Odoy S, Fujiwara H, Hasegawa M, Iwatsubo T, Trojanowski JQ, Kretzschmar HA, Haass C (2002) Misfolded proteinase K-resistant hyperphosphorylated alpha-synuclein in aged transgenic mice with locomotor deterioration and in human alpha-synucleinopathies. J Clin Invest 110:1429–1439.

Polymeropoulos MH, Lavedan C, Leroy E, Ide SE, Dehejia A, Dutra A, Pike B, Root H, Rubenstein J, Boyer R, Stenroos ES, Chandrasekharappa S, Athanassiadou A, Papapetropoulos T, Johnson WG, Lazzarini AM, Duvoisin RC, Di Iorio G, Golbe LI, Nussbaum RL (1997) Mutation in the alpha-synuclein gene identified in families with Parkinson's disease. Science 276:2045–2047.

Richfield EK, Thiruchelvam MJ, Cory-Slechta DA, Wuertzer C, Gainetdinov RR, Caron MG, Di Monte DA, Federoff HJ (2002) Behavioural and neurochemical effects of wild-type and mutated human alpha-synuclein in transgenic mice. Exp Neurol 175:35–48.

Rockenstein E, Mallory M, Hashimoto M, Song D, Shults CW, Lang I, Masliah E (2002) Differential neuropathological alterations in transgenic mice expressing alpha-synuclein from the platelet-derived growth factor and Thy-1 promoters. J Neurosci Res 68:568–578.

Sambrook J, Russell DW (2001) Calcium-phosphate-mediated transfection of eukaryotic cells with plasmid DNAs. In: Molecular cloning: A laboratory manual, third ed. (Irwin N, Janssen KA, eds), pp 16.14–16.20. New York: Cold Spring Harbor Laboratory Press.

Shen Y, Muramatsu SI, Ikeguchi K, Fujimoto KI, Fan DS, Ogawa M, Mizukami H, Urabe M, Kume A, Nagatsu I, Urano F, Suzuki T, Ichinose H, Nagatsu T, Monahan J, Nakano I, Ozawa K (2000) Triple transduction with adeno-associated virus vectors expressing tyrosine hydroxylase, aromatic-L-amino-acid decarboxylase, and GTP cyclohydrolase I for gene therapy of Parkinson's disease. Hum Gene Ther 11:1509–1519.

Shimura H, Hattori N, Kubo S, Mizuno Y, Asakawa S, Minoshima S, Shimizu N, Iwai K, Chiba T, Tanaka K, Suzuki T (2000) Familial Parkinson disease gene product, parkin, is a ubiquitin-protein ligase. Nat Genet 25:302–305.

Singleton AB, Farrer M, Johnson J, Singleton A, Hague S, Kachergus J, Hulihan M, Peuralinna T, Dutra A, Nussbaum R, Lincoln S, Crawley A, Hanson M, Maraganore D, Adler C, Cookson MR, Muenter M, Baptista M, Miller D, Blancato J, Hardy J, Gwinn-Hardy K (2003) Alpha-synuclein locus triplication causes Parkinson's disease. Science 302:841.

Spillantini MG, Schmidt ML, Lee VM, Trojanowski JQ, Jakes R, Goedert M (1997) Alpha-synuclein in Lewy bodies. Nature 388: 839–840.

van der Putten H, Wiederhold KH, Probst A, Barbieri S, Mistl C, Danner S, Kauffmann S, Hofele K, Spooren W, Ruegg MA, Lin S, Caroni P, Sommer B, Tolnay M, Bilbe G (2000) Neuropathology in mice expressing human alpha-synuclein. J Neurosci 20:6021–6029.

Xu J, Kao SY, Lee FJ, Song W, Jin LW, Yankner BA (2002) Dopamine-dependent neurotoxicity of alpha-synuclein: A mechanism for selective neurodegeneration in Parkinson disease. Nat Med 8: 600–606.

Yamada M, Iwatsubo T, Mizuno Y, Mochizuki H (2004) Overexpression of alpha-synuclein in rat substantia nigra results in loss of dopaminergic neurons, phosphorylation of alpha-synuclein and activation of caspase-9: resemblance to pathogenetic changes in Parkinson's disease. J Neurochem 91:451–461.

Yamada M, Mizuno Y, Mochizuki H (2005) Parkin gene therapy for alpha-synucleinopathy: a rat model of Parkinson's disease. Hum Gene Ther 16:262–270.

Yao D, Gu Z, Nakamura T, Shi ZQ, Ma Y, Gaston B, Palmer LA, Rockenstein EM, Zhang Z, Masliah E, Uehara T, Lipton SA (2004) Nitrosative stress linked to sporadic Parkinson's disease: *S*-nitrosylation of parkin regulates its E3 ubiquitin ligase activity. Proc Natl Acad Sci U S A 101:10810–10814.

Zarranz JJ, Alegre J, Gomez-Esteban JC, Lezcano E, Ros R, Ampuero I, Vidal L, Hoenicka J, Rodriguez O, Atares B, Llorens V, Gomez-Tortosa E, del Ser T, Munoz DG, de Yebenes JG (2004) The new mutation, E46K, of alpha-synuclein causes Parkinson and Lewy body dementia. Ann Neurol 55:164–173.

(Accepted 21 September 2006)
(Available online 13 November 2006)

Available online at www.sciencedirect.com
ScienceDirect
Neuroscience Research 57 (2007) 550–558
Neuroscience Research
www.elsevier.com/locate/neures

Differential characteristics of HIV-based versus SIV-based lentiviral vector systems: Gene delivery to neurons and axonal transport of expressed gene

Ryo Kitagawa [a], Shigehiro Miyachi [b,c], Hideki Hanawa [a], Masahiko Takada [b,c,*], Takashi Shimada [a]

[a] *Department of Biochemistry and Molecular Biology, Nippon Medical School, Tokyo 113-8602, Japan*
[b] *Department of System Neuroscience, Tokyo Metropolitan Institute for Neuroscience, Fuchu, Tokyo 183-8526, Japan*
[c] *CREST, Japan Science and Technology Corporation, Kawaguchi, Saitama 332-0012, Japan*

Received 22 September 2006; accepted 26 December 2006
Available online 10 January 2007

Abstract

The differential characteristics of lentiviral vectors based on human and simian immunodeficiency viruses (HIV and SIV) were investigated in rats and monkeys. Each vector was injected into the striatum, and the expression patterns of the marker gene green fluorescent protein (GFP) were analyzed in the basal ganglia. With respect to the capability of gene delivery to neural cells, the HIV-based vector exhibited a higher tropism to neurons than to astroglias in the striatum, and vice versa for the SIV-based vector. The preferential direction of axonal transport of striatally expressed GFP was also examined in the present study. The HIV-based vector allowed for both anterograde transport via the striatopallidal and striatonigral pathways and retrograde transport via the nigrostriatal pathway. The GFP labeling of axon terminals through anterograde transport was apparent regardless of the animal species, while that of neuronal cell bodies through retrograde transport was much more prominent in monkeys than in rats. As for the SIV-based vector, on the other hand, evidence for anterograde transport was obtained much more markedly in monkeys than in rats, and only weak or no retrograde transport occurred in either monkeys or rats. Our results indicate that HIV-based, but not SIV-based, lentiviral vectors possess the high tropism to neurons and permit retrograde transport of an expressed gene, especially in primates. The latter property might carry a potential benefit in gene therapy for Parkinson's disease, as stereotaxic injections of the vectors could be performed into the striatum, spatially larger than the substantia nigra, with greater certainty.

Keywords: Basal ganglia; Dopamine; Lentivirus; Parkinson's disease; Striatum; Substantia nigra

1. Introduction

For the purpose of laboratory experiments and gene therapy trials, emphasis has been placed on the development of viral vectors. The use of neurotropic viruses is essential to transfer genes into neural cells, and, therefore, vectors based on such viruses (e.g., adenovirus, adeno-associated virus) have extensively been applied to a variety of studies (Stedman et al., 2000; Ferrarese et al., 2001; Janson et al., 2002; Crystal et al., 2004; Nakao et al., 2004; Tuszynski et al., 2005). Among the neurotropic viruses, a family of lentiviruses has increasingly been regarded as a potent candidate to achieve a vector system that allows for the stable and long-term delivery of genes to discrete brain regions (Volsky et al., 1992; Naldini et al., 1996; Mochizuki et al., 1998; Kordower et al., 1999; Baekelandt et al., 2002; Lai and Brady, 2002; Scherr et al., 2002; Dowd et al., 2005; Kyrkanides et al., 2005; Wong et al., 2005). The lentiviruses exhibit slow, non-oncogenetic pathogenesis and complex genomic organization. According to their sequence similarities, the lentiviruses can be classified into primate and non-primate types. The former type is composed of human and simian immunodeficiency viruses (HIV and SIV), and the latter type includes a number of viruses, e.g., feline and bovine immunodeficiency viruses, equine infectious anaemia virus.

* Corresponding author at: Department of System Neuroscience, Tokyo Metropolitan Institute for Neuroscience, Tokyo Metropolitan Organization for Medical Research, Fuchu, Tokyo 183-8526, Japan.
Tel.: +81 42 325 3881; fax: +81 42 321 8678.
E-mail address: takada@tmin.ac.jp (M. Takada).

0168-0102/$ – see front matter
doi:10.1016/j.neures.2006.12.016

Since HIV type 1 (HIV-1) is the best characterized of the lentiviruses, major interest has focused on establishing vector systems derived from HIV-1. In fact, HIV-1-based lentiviral vectors have been shown to transduce various non-dividing cells in the brain *in vivo* (Kordower et al., 1999; Bensadoun et al., 2000; Déglon et al., 2000; Baekelandt et al., 2002; Marr et al., 2003; Rosenblad et al., 2003; Georgievska et al., 2004; Lo Bianco et al., 2004; Popovic et al., 2005; Sajadi et al., 2005; Brizard et al., 2006). With respect to the therapeutic use for Parkinson's disease, it has been reported that the HIV-1-based vectors can be delivered to the striatum and the substantia nigra in non-human primates where the marker gene β galactosidase is expressed predominantly in neurons and, to a lesser extent, in astroglias (Kordower et al., 2000). Moreover, the safety and efficiency of gene transfer by the HIV-1-based vectors have been evaluated in the same work.

Although characterization of HIV-1-based lentiviral vectors and evaluation of their delivery systems have been well documented, knowledge of SIV-based lentiviral vectors has so far been limited. Characterization of these vectors derived from SIV has demonstrated that they are similar to those derived from HIV-1 or HIV type 2 in terms of the insertion of transgenes into non-proliferating cells. It has been thought that SIV-based vectors have better efficiency of gene delivery than HIV-1-based vectors in simian cells (Nègre and Cosset, 2002), thus implying that they may provide a valid candidate alternative to HIV-1-based vectors. Recently, Hanawa et al. (2004) has tested a vector system derived from $SIVmac_{1A11}$, a non-pathogenic lentivirus that was obtained from the National AIDS Reagent Repository (Washington, DC, USA). This SIV-based vector was developed by replacing the HIV-1 sequences with the corresponding segments of the $SIVmac_{1A11}$ plasmid. In the present study, we therefore analyzed the differential properties of the HIV-1-derived versus $SIVmac_{1A11}$-derived vector systems by injecting each vector into the striatum of both rats and monkeys. First, the capacities to be delivered to neural cells (neurons versus astroglias) were compared between the two vectors. Second, the preferential direction of axonal transport (anterograde versus retrograde) was investigated for the reporter gene green fluorescent protein (GFP) that was delivered to neurons by the vectors. In contrast with the high efficiency of their gene transfer into neural cells, HIV-1-based vectors have been shown to transduce hematopoietic stem cells only so poorly in monkeys (Hanawa et al., 2004). This is ascribed to the enrichment of TRIM5α, an inhibitory protein for HIV-1 infection, in the blood (Stremlau et al., 2004; Song et al., 2005). Thus, we examined the content of TRIM5α in the brain compared with that in the blood.

2. Materials and methods

2.1. Experimental animals

Four female Wistar rats (150–250 g b.wt.) and three female crab-eating monkeys (*Macaca fascicularis*; 2.5–3.5 kg b.wt.) were used for this study. The entire experiments with intrastriatal injections of lentiviral vectors were carried out in a special laboratory (biosafety level 2) designated for *in vivo* infectious experiments. Throughout the experiments, the rats were kept inside a small safety cabinet, and the monkeys were kept in individual cages that were placed inside a special safety cabinet. The experimental protocol was approved by the Animal Care and Use Committee of the Tokyo Metropolitan Institute for Neuroscience, and all experiments were conducted according to the Guideline for the Care and Use of Animals (Tokyo Metropolitan Institute for Neuroscience 2000).

2.2. Lentiviral vectors

Two types of lentiviral vectors, an HIV-1-based transfer vector encoding GFP (pCL20c MSCV-GFP; HIV-GFP) and a $SIVmac_{1A11}$-based transfer vector encoding GFP (pCL20cSLFR MSCV-GFP; SIV-GFP), were used in the present *in vivo* experiments. Constructions of these vectors were described elsewhere (Hanawa et al., 2004), although a conditioned medium containing vector particles was produced with minor modifications. Briefly, 3×10^6 293T cells were seeded onto 10 cm dishes, kept in place for 24 h, and then transfected with a total of 20 μg DNA composed as follows: 6 μg pCAGkGP1.1R (or pCAG-SIVgprre), 2 μg pCAG4-RTR2 (or pCAG4-RTR-SIV), 2 μg pCAG-VSV-G, and 10 μg pCL20c MSCV-GFP (or pCL20cSLFR MSCV-GFP). Eighteen hours after transfection, the 293T cells were washed in 0.1 M phosphate-buffered saline (PBS; pH 7.4) twice and overlaid with 7 ml/dish of Dulbecco modified eagle medium supplemented with 10% fetal bovine serum, 50 U/ml penicillin G, 50 μg/ml streptomycin, and 1×MEM non-essential amino acid solution (D10; Sigma–Aldrich, St. Louis, MO, USA). After 12 h incubation, the conditioned medium containing vector particles was harvested and stored in a 4 °C refrigerator. The transfected 293T cells were overlaid with 7 ml of D10 and conditioned medium was harvested 12 h later again. The conditioned media harvested at different time points were combined, cleared by low-speed centrifugation, filtered, and then concentrated about 250-folds in volume by ultracentrifugation in a swinging bucket rotor (SW28; Beckman Coulter Inc., Fullerton, CA, USA) at 25,000 rpm for 90 min at 4 °C. The concentrates were snap frozen in aliquots, and stored at −80 °C. The HIV-GFP and SIV-GFP were titered by transducing HeLa cells with serial dilutions. Briefly, 5×10^4 HeLa cells were seeded into 6-well Plates 24 h before transduction, and the transduction was performed in the presence of 8 μg/ml of polybrene. After 3–4 days additional culture, the transduction rate is estimated using flow cytometry (FACSCalibur; BD Biosciences, Franklin Lakes, NJ, USA). The titer was routinely determined from a volume of a vector preparation that yielded linear, dose-dependent transduction of target cells at a level of less than 20%.

2.3. Surgical procedures and injections of viral vectors

Under general anesthesia with sodium pentobarbital (25 mg/kg, i.p.), rats were positioned in a stereotaxic frame. The skull was widely exposed, and a small portion of the skull over the striatum was removed with a dental drill. Subsequently, 5 μl of each of the vector preparations (1.5×10^9 TU/ml) was injected into the striatum through a 10-μl Hamilton microsyringe. In two of four rats, single injection of HIV-GFP or SIV-GFP was made on one side of the brain. In the other two rats, HIV-GFP injections were made on one side, and SIV-GFP injections were made symmetrically on the opposite side of the brain.

In two of three monkeys, intrastriatal injections of the viral vectors were performed. The monkeys were first sedated with ketamine hydrochloride (5 mg/kg, i.m.) and xylazine hydrochloride (0.5 mg/kg, i.m.), and then anesthetized with sodium pentobarbital (20 mg/kg, i.v.). They were seated in a primate chair with their head fixed in a stereotaxic frame attached to the chair. After partial removal of the skull, multiple injections of HIV-GFP were made into the unilateral putamen, and those of SIV-GFP were made contralaterally. A total of 50 μl of each vector preparation (1.5×10^9 TU/ml) was injected at five rostrocaudally different levels (10 μl each) through a 50-μl Hamilton microsyringe.

2.4. Histological procedures

After survival periods of 24–25 days, the rats and monkeys were anesthetized deeply with sodium pentobarbital (50 mg/kg, i.p.) and perfused transcardially with PBS, followed by a mixture of 8% formalin and 15% saturated picric acid in 0.1 M phosphate buffer (PB; pH 7.4). The brains were removed from the

skull, postfixed in the same fresh fixative overnight, and immersed in PB containing 30% sucrose until they sank. Coronal sections were cut serially at 40 μm thickness for the rat brain and at 60 μm thickness for the monkey brain on a freezing microtome.

The sections were divided into six groups. The first group of the sections was immunohistochemically processed for GFP. Every sixth section was washed in PBS, soaked with 1% skim milk in PBS, and then incubated overnight with rabbit anti-GFP antibody (diluted at 1:2000; Molecular Probes, Eugene, OR, USA) dissolved in a PBS medium containing 1% normal goat serum and 0.1% Triton X-100. Subsequently, the sections were incubated for 2 h in the same fresh medium containing biotinylated goat anti-rabbit IgG antibody (diluted at 1:200; Vector Laboratories, Burlingame, CA, USA), followed by avidin–biotin–peroxidase complex (ABC Elite; Vector Laboratories) for another 2 h. For visualization of the antigen, the sections were reacted in 0.05 M Tris–HCl buffer (pH 7.6) containing 0.04% diaminobenzidine (DAB), 0.04% nickel chloride, and 0.002% hydrogen peroxide. The sections were mounted onto gelatin-coated glass slides, air-dried, and then coverslipped.

Other groups of the sections were processed for double immunofluorescence histochemistry for GFP and one of the following substances: NeuN, glial fibrillary acid protein (GFAP), and tyrosine hydroxylase (TH). Briefly, the sections were incubated overnight with a cocktail of the rabbit anti-GFP antibody (diluted at 1:2000; Molecular Probes) and one of the following primary antibodies: mouse monoclonal anti-NeuN antibody (diluted at 1:5000; Chemicon, Temecula, CA, USA), mouse monoclonal anti-GFAP antibody (diluted at 1:500; Sigma, St. Louis, MO, USA), and mouse monoclonal anti-TH antibody (diluted at 1:2000; Chemicon). They were incubated for 2 h with biotinylated goat anti-mouse IgG antibody (diluted at 1:200; Vector Laboratories), then with Cy3 (diluted at 1:200; Jackson Immuno Research, Grove, PA, USA) for 1 h, and, finally, with Alexa Fluor 488 donkey anti-rabbit IgG antibody (diluted at 1:100; Molecular Probes) for 2 h. The sections were observed under a confocal laser-scanning microscope (Leica Microsystems, Tokyo, Japan). Other technical details were as described above.

2.5. Data analysis

In a series of DAB-reacted sections, the number of GFP-positive cells in the substantia nigra was counted in every sixth section (240 μm apart for rats and 360 μm apart for monkeys), and the average of the data in two rats (with bilateral injections) or two monkeys was obtained for HIV-GFP and SIV-GFP. For counting striatal cells double-immunostained for GFP, NeuN, and GFAP, images taken with a fluorescent microscope system (Biozero; Keyence, Osaka, Japan) were printed. From representative sections through the injection sites of each vector, six or ten square areas (200 μm × 200 μm) around the injection needle tracks were randomly selected for rats or monkeys, respectively. Cell counts were done in these areas, and the ratio of NeuN-positive or GFAP-positive cells to the total GFP-positive cells and the ratio of GFP-positive cells to the total NeuN-positive or GFAP-positive cells were calculated. The ratio of NeuN-positive cells to GFAP-positive cells was also calculated. Then, the average of the data in two rats (with bilateral injections) or two monkeys was obtained for HIV-GFP and SIV-GFP.

2.6. Reverse transcriptase polymerase chain reaction (RT-PCR)

The remaining monkey was anesthetized deeply with sodium pentobarbital (50 mg/kg, i.p.) and perfused transcardially with 0.1 M PBS. The brain was immediately removed from the skull, and some tissue was obtained from the striatum. Total RNAs were isolated not only from the brain, but also from the blood (collected before perfusion) by using RNA Preparation Kit (Qiagen, Hilden, Germany) or TRIzol® Reagent (Invitrogen, Carlsbad, CA, USA). In the reverse transcription reaction, cDNAs were synthesized from 200 ng of mRNA (a total volume of 20 μl). Using 10 μl of this 20-μl reverse transcription product, the DNAs for monkey TRIM5α were amplified with the primers 5′-TCA CTG CGA ACC ACA AGA AG-3′ and 5′-GCT CAC AAA GCC AGC AAA TG-3′, while using the remaining 10 μl of the product, the DNAs for β-actin were amplified with the primers 5′-CAT TGT GAT GGA CTC CGG AGA CGG-3′ and 5′-CAT CTC CTG CTC GAA GTC TAG AGC-3′ by using TAKARA RNA PCR Kit (AMV; Ver. 3.0). Thermocycling reactions of PCR were carried out as follows: (1) 95 °C for 30 s; (2) 30 cycles of 95 °C for 30 s, 55 °C for 1 min, and 72 °C for 1 min; (3) 68 °C for 5 min. The RT-PCR products were visualized with Gel Documentation System (AE-6911FXFD; ATTO & Rise Corporation, Tokyo, Japan) and analyzed quantitatively with CS Analyzer (ATTO & Rise Corporation).

For more quantitative analysis, the reverse transcription was performed by using Reverse Transcription Reagents (Applied Biosystems, Foster City, CA, USA), and the PCR reaction was performed by using SYBR® Premix Ex Taq™ (Takara Bio Inc., Otsu, Japan) and ABI PRISM 7700 (Applied Biosystems). The primer sets used to amplify TRIM5α and β-actin transcripts were as described above. The relative quantity of TRIM5α in the brain was determined by using the standard curve method. The Ct value of 50 ng of brain RNA was compared with those of a series of diluted blood RNAs (50 ng, 10 ng, 2 ng, and 0.4 ng), and the corresponding amount (ng in blood RNA) was determined. Finally, the determined TRIM5α level was normalized with the β-actin level.

3. Results

3.1. GFP delivery to rat striatum by HIV-1 and SIV

Injections of HIV-GFP and SIV-GFP were made into the striatum. The titer and volume of SIV-GFP were the same as those of HIV-GFP. When these vectors were injected in single rats, intrastriatal injection of each vector was made symmetrically on one side or another. The site of HIV-GFP injection encompassed the striatum rather extensively, and the site of SIV-GFP injection involved a slightly smaller area (Fig. 1A and B). As there was no evidence for vector transfer between hemispheres in the case of unilateral injections, only the data obtained in two rats with bilateral injections were analyzed here. First, we examined the extent to which GFP was delivered to striatal cells (neurons versus astroglias) by these vectors. With respect to the HIV-1 vector, more than 2/3 of striatal cells expressing GFP were immunostained for the neuronal marker NeuN, while less than 30% of them were immunostained for the astroglial marker GFAP (Table 1). On the side injected with the SIV vector, only 7.7% of GFP-expressing cells were immunoreactive for NeuN, whereas more than half of them were immunoreactive for GFAP (Table 1). When the GFP-expressing cells were viewed from the ratio to the total striatal cells displaying NeuN or GFAP immunoreactivity within the injection sites, 21.7% of NeuN-immunoreactive cells and 9.5% of GFAP-immunoreactive cells expressed GFP on the side injected with the HIV-1 vector (Table 1). With respect to the SIV vector, only 1.1% of NeuN-positive cells expressed GFP, although the ratio of GFP-expressing cells to GFAP-positive cells was equivalent to that for the HIV-1 vector (Table 1). No inflammatory cell invasion was seen except areas along the injection needle tracks.

Next, we investigated the preferential direction of axonal transport (anterograde direction from cell bodies to terminals versus retrograde direction from terminals to cell bodies) of GFP delivered to striatal neurons by the HIV-1 and SIV vectors. On the side ipsilateral to the HIV-GFP injection, accumulations of axon terminals immunolabeled for GFP were densely observed in the globus pallidus, the entopeduncular nucleus, and the substantia nigra pars reticulata (SNr), each of which is a major target for output from the striatum (Fig. 1C–E). This indicates the occurrence of anterograde transport of the striatally expressed GFP. By contrast, only sparse terminal

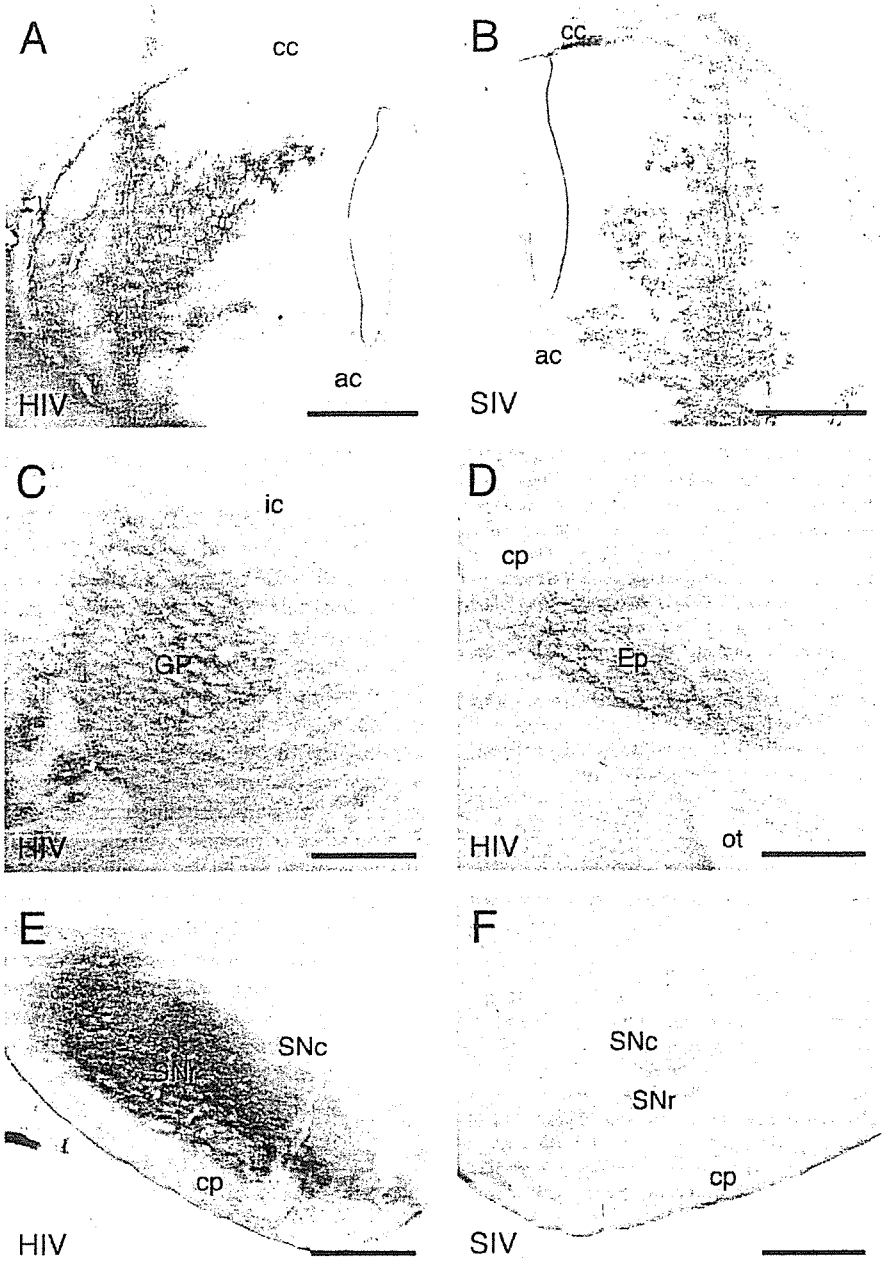

Fig. 1. (A) Injection site of HIV-GFP in the rat striatum. (B) Injection site of SIV-GFP in the striatum on the contralateral side. (C) Anterograde labeling in the globus pallidus (GP) after the HIV-GFP injection. (D) Anterograde labeling in the entopeduncular nucleus (Ep) after the HIV-GFP injection. (E) Anterograde labeling in the substantia nigra pars reticulata (SNr) after the HIV-GFP injection. (F) Anterograde labeling in the SNr after the SIV-GFP injection. ac, anterior commissure; cc, corpus callosum; cp, cerebral peduncle; ic, internal capsule; ot, optic tract; SNc, substantia nigra pars compacta. Scale bars, 1 mm for (A) and (B), 500 μm for (C)–(F).

Table 1
Relationships between GFP-positive cells and NeuN/GFAP-positive cells in the striatum

	% GFP + NeuN/total GFP	% GFP + GFAP/total GFP	% NeuN + GFP/total NeuN	% GFAP + GFP/total GFAP	% Neuron/Glia
Rats					
HIV-GFP	67.7	22.1	21.7	9.5	3.82
SIV-GFP	7.7	51.6	1.1	9.9	0.25
Monkeys					
HIV-GFP	50.8	38.3	16.7	14.4	1.50
SIV-GFP	15.0	48.6	5.0	14.8	0.37

Table 2
Number of retrogradely labeled neurons in SNc[a]

	HIV-GFP	SIV-GFP
Rats	8	0
Monkeys	333	14

[a] Data represent the average of the number of GFP-positive cells in two cases. In each case, cell counts were done in every sixth section.

labeling was found on the side ipsilateral to the SIV-GFP injection (Fig. 1F). In addition, a small number of GFP-labeled neurons (eight cells obtained from every sixth section; Table 2) were seen in the substantia nigra pars compacta (SNc) after the HIV-GFP injection. All of these neurons were double-immunostained for TH, the initial and rate-limiting enzyme of dopamine synthesis (data not shown). This is certainly attributed to retrograde transport from the striatum where GFP was primarily expressed. However, no such neuronal labeling was virtually detected in the SNc after the SIV-GFP injection (Table 2).

3.2. GFP delivery to monkey striatum by HIV-1 and SIV

In two monkeys, intrastriatal injections of HIV-GFP and SIV-GFP were made symmetrically at five rostrocaudally different levels of each hemisphere. The injection sites of these vectors were placed in the dorsal portions of the putamen (Fig. 2A). When we analyzed the proportion of NeuN-immunoreactive or GFAP-immunoreactive cells to the total striatal cells expressing GFP, the former was 50.8% and the latter was 38.3% on the side injected with the HIV-1 vector (Table 1; see also Fig. 3A and B). On the side injected with the SIV vector, 15.0% of GFP-expressing cells were immunostained for NeuN, while 48.6% of them were immunostained for GFAP (Table 1; see also Fig. 3C and D). On the other hand, the proportion of GFP-expressing cells to the total NeuN-positive or GFAP-positive cells within the striatal injection sites was 16.7% or 14.4%, respectively, on the side injected with the HIV-1 vector (Table 1). On the side injected with the SIV vector, only 5.0% of NeuN-positive cells expressed GFP, although the proportion of GFP-expressing cells to GFAP-positive cells was almost the same as that for the HIV-1 vector (Table 1).

In terms of GFP labeling via axonal transport, dense accumulations of axon terminals were seen in the external and internal segments of the globus pallidus and SNr on the side ipsilateral to the HIV-GFP injection (Fig. 2A and B). Similar findings, indicative of anterograde transport of the striatally expressed GFP, were obtained on the side ipsilateral to the SIV-GFP injection (Fig. 2C). Moreover, a large number of GFP-labeled neurons (333 cells obtained from every sixth section; Table 2) were observed in the SNc after the HIV-GFP injection into the putamen (Fig. 2B). After the SIV-GFP injection, on the other hand, much fewer neurons (14 cells obtained from every sixth section; Table 2) were labeled in the SNc through retrograde transport from the injection site (Fig. 2C). Again, no

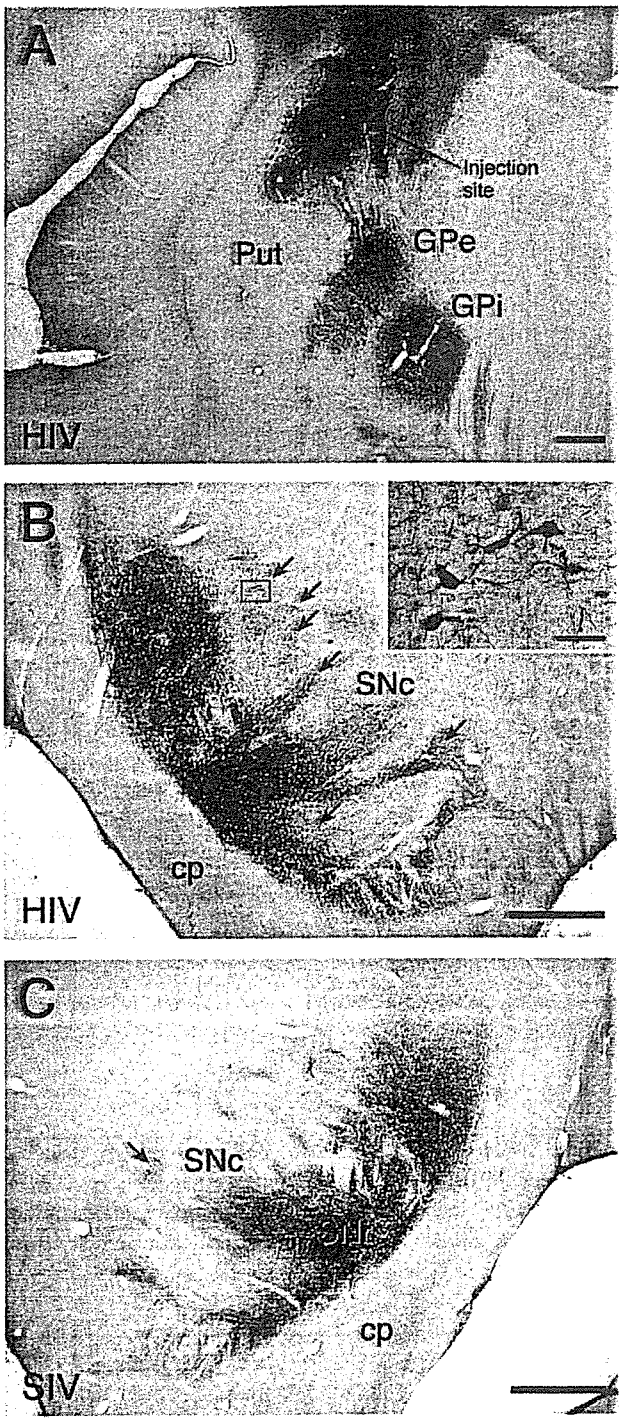

Fig. 2. (A) Injection site of HIV-GFP in the monkey putamen (Put) and anterograde labeling in the external (GPe) and internal (GPi) segments of the globus pallidus. (B) Anterograde labeling in the substantia nigra pars reticulata (SNr) and retrograde labeling (arrows) in the substantia nigra pars compacta (SNc) after the HIV-GFP injection. (Inset) Higher-power magnification of the rectangular area. (C) Anterograde labeling in the SNr after the SIV-GFP injection into the putamen on the contralateral side. Only a few retrogradely labeled neurons (arrow) are seen in the SNc. cp, cerebral peduncle. Scale bars, 1 mm for (A)–(C), 50 μm for inset in (B).

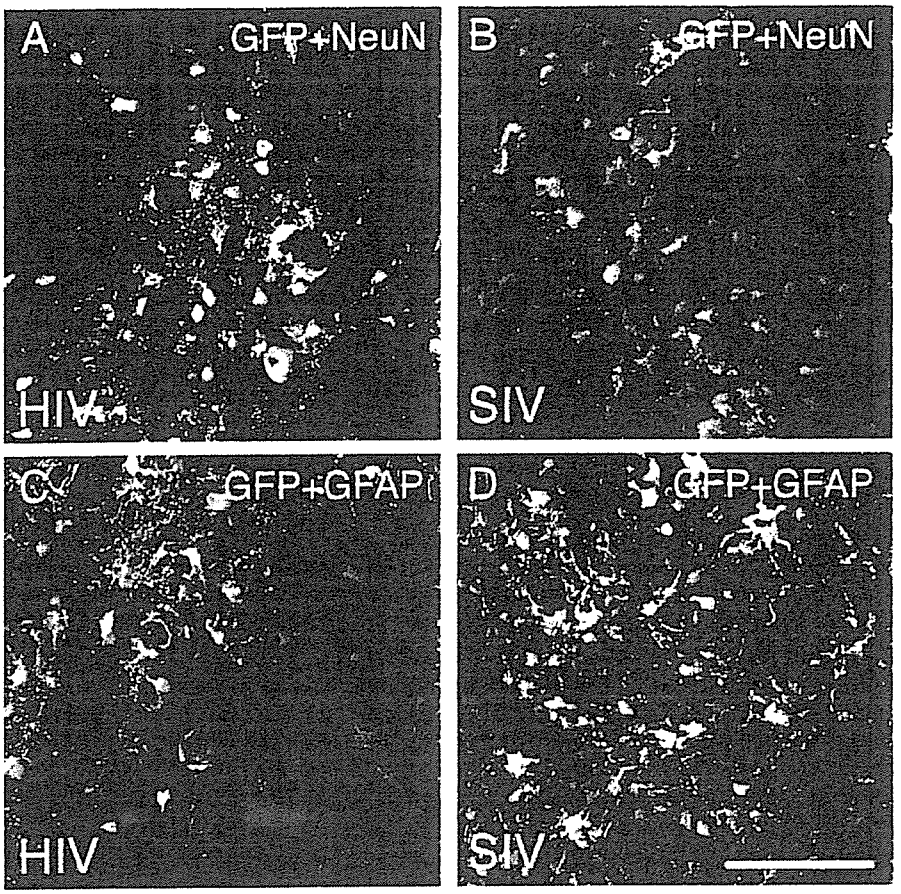

Fig. 3. Striatal cells immunoreactive for GFP and NeuN/GFAP in the vicinity of the injection sites of HIV-GFP and SIV-GFP in the monkey putamen. (A) GFP (green) and NeuN (red) immunoreactivities after the HIV-GFP injection. (B) GFP (green) and NeuN (red) immunoreactivities after the SIV-GFP injection. (C) GFP (green) and GFAP (red) immunoreactivities after the HIV-GFP injection. (D) GFP (green) and GFAP (red) immunoreactivities after the SIV-GFP injection. Scale bar, 100 μm for (A)–(D).

apparent invasion of inflammatory cells was observed except areas along the injection needle tracks.

Our double immunofluorescence histochemical staining revealed that on the side injected with the HIV-1 vector, substantially all GFP-positive neurons in the SNc were immunoreactive for TH (Fig. 4A–A″). We further confirmed that many of presumed GFP-positive axon terminals in the putamen on the same side displayed TH immunoreactivity (Fig. 4C). By contrast, neither GFP-positive neurons in the SNc nor GFP-positive axon terminals in the putamen were dominantly found on the side injected with the SIV vector (Fig. 4B–B″ and D).

3.3. RT-PCR analyses

To compare the content of TRIM5α between the brain and the blood, RT-PCR analyses were performed. The TRIM5α cDNAs were synthesized and amplified with mRNAs isolated from the brain (striatal tissue) and blood. Six sets of the TRIM5α cDNAs (approximately 1500 bps) were made with the copy number from 1.0×10^2 to 1.0×10^7. These sets of the cDNAs and mRNAs from the brain and blood were amplified at the same time. On the gradation of the cDNA sets, the copy number of blood mRNAs was 3.7×10^3. The copy number of brain mRNAs, on the other hand, was 2.9×10^2 (Fig. 5). The density volume of β-actin from the blood or brain was 8.6×10^4 or 4.9×10^4, respectively, after the same PCR cycles (Fig. 5). Thus, the copy number of TRIM5α mRNAs from the blood was 7.3-fold of that from the brain by correcting with the density volume of β-actin.

In the quantitative RT-PCR, the amount of TRIM5α mRNA in 50 ng of the total RNA obtained from the brain sample was equivalent to that in 7.6 ng of the total RNA obtained from the blood sample. This indicates that the TRIM5α mRNA level in the brain is only 15% as much as in the blood. On the other hand, the amount of β-actin mRNA in 50 ng of the same brain sample was equivalent to that in 19 ng of the total blood RNA. If it is assumed that the β-actin level in the brain is identical to that in the blood, the normalized TRIM5α expression level in the brain is approximately 40% of that in the blood (data not shown).

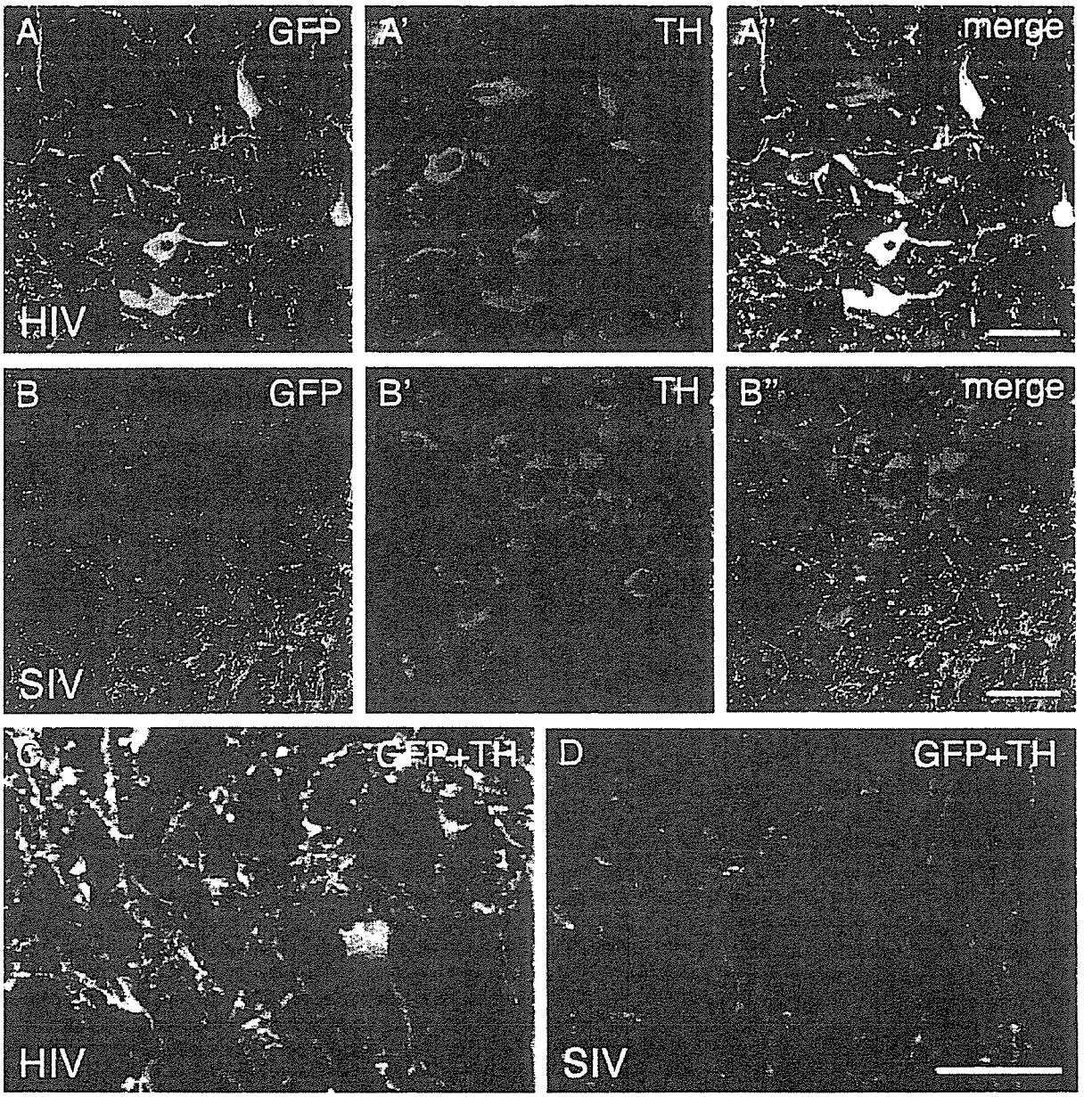

Fig. 4. (A–A″) TH immunoreactivity (red) of nigral neurons expressing GFP (green) after the intrastriatal HIV-GFP injection in the monkey. (B–B″) TH immunoreactivity (red) of nigral neurons expressing GFP (green) after the intrastriatal SIV-GFP injection. (C) TH immunoreactivity (red) of striatal terminals expressing GFP (green) after the intrastriatal HIV-GFP injection. (D) TH immunoreactivity (red) of striatal terminals expressing GFP (green) after the intrastriatal SIV-GFP injection. Scale bars, 50 μm for (A–A″) and (B–B″), 100 μm for (C) and (D).

4. Discussion

The present results define that the HIV-1-based and SIV-based lentiviral vectors are differentially characterized in both rats and monkeys. With respect to the capability of gene delivery to neural cells, there exists a marked difference between the two vectors. As indicated in Table 1 (see % Neuron/Glia), the HIV-1-based vector displays a greater tropism to neurons than to astroglias in the striatum (see also Déglon et al., 2000), and vice versa for the SIV-based vector. This differential tropism of each vector to neurons versus astroglias is common to both rats and monkeys. Furthermore, analysis of the ratio of GFP-expressing cells to NeuN-positive or GFAP-positive striatal cells has shown that the HIV-1-based vector exhibits a much higher tropism to neurons than the SIV-based one irrespective of the animal species, while both vectors retain almost the same transduction efficiency to astroglias (see Table 1). It is surprising that the HIV-1-based lentiviral vector transfers the GFP gene efficiently into striatal cells of macaque monkeys, given that TRIM5α which is enriched in monkey blood tissue largely prevents hematopoietic stem cells

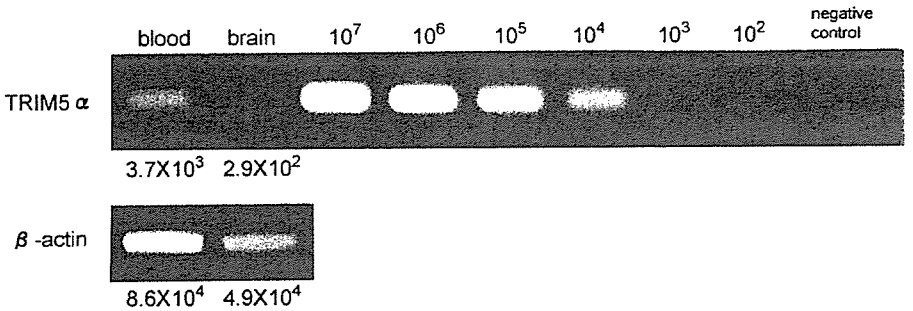

Fig. 5. RT-PCR for the content of TRIM5α and β-actin in the monkey blood and brain. The copy number of TRIM5α mRNAs from the blood was 7.3-fold of that from the brain by correcting with the density volume of β-actin.

from HIV-1 infection (Stremlau et al., 2004). Since this inhibitory protein for reverse transcription of HIV-1 exerts little influence on SIV infection, SIV-based vectors can transduce hematopoietic stem cells more effectively than HIV-1-based ones (Hanawa et al., 2004). Therefore, the content of TRIM5α in the monkey brain was determined by RT-PCR, in comparison with that in the blood. Our data have demonstrated that the expression level of TRIM5α is much lower in the brain (striatal tissue) than in the blood, which allows for the high efficiency of gene transfer into neural cells, especially into neurons, by the HIV-1-based vector.

A previous work has briefly reported the occurrence of anterograde and retrograde transport of a marker gene that was delivered to the monkey striatum by an HIV-1-based vector (Kordower et al., 2000). It has been revealed in the present study that the preferential direction exists in axonal transport of the GFP gene expressed in neurons by means of the HIV-1-based and SIV-based lentiviral vectors. As for the HIV-1-based vector, axon terminals in output targets for the striatum were labeled with GFP via anterograde transport along the striatopallidal and striatonigral pathways. Such terminal labeling was explicitly detected in both rats and monkeys. Moreover, GFP labeling of neuronal cell bodies via retrograde transport occurred in the SNc along the nigrostriatal dopaminergic pathway. This event was much more prominent in monkeys than in rats, although the number of labeled dopaminergic neurons was even small as compared to conventional retrograde tracings. In the case of the SIV-based vector, on the other hand, evidence for anterograde transport of GFP along the striatopallidal and striatonigral pathways was obtained much more markedly in monkeys than in rats. Only weak or no retrograde transport of GFP along the nigrostriatal dopaminergic pathway appeared to take place in either monkeys or rats. It still remains a mystery why retrograde transport of the reporter gene is not readily permitted regardless of the vector type or animal species. This could be accounted for by postulating that the extent of viral infection to and/or viral uptake from axon terminals may be different from that for anterograde transport from neuronal cell bodies, as indicated by the distinct patterns of GFP labeling of dopaminergic terminals in the striatum (see Fig. 4C and D).

As described above, the HIV-1-based lentiviral vector displays a greater efficiency of gene delivery to neurons than the SIV-based one. In view of the fact that the titer of the HIV-1-based vector was equivalent to that of the SIV-based vector, this may depend on the potential of each vector to transfer genes into neurons. Although both the HIV-1-based and the SIV-based vectors were prepared in the paralleled vector production system (Hanawa et al., 2004) and these titers were adjusted to the same level (1.5×10^9 TU/ml) prior to use, the original titer of the former was 1.2×10^{10} TU/ml that was eight times as high as that of the latter. The use of the original SIV-based vector may cause contamination of a large amount of cell membrane debris, which can inhibit transduction of neurons into SIV-based vector preparations. If the neurons have a smaller amount of receptors for VSV-G, then a higher amount of cell membrane contaminant from VSV-G transfected 293T cells can exert a deteriorating effect on those neurons. Moreover, the SIV-based vector we used might have attenuated infection efficiency in the process of reverse transcription and/or cytoplasm-nucleus transport. Further investigations, however, are needed to address this issue.

Unlike oncoretroviruses, lentiviruses are capable of transducing various non-dividing cells in the brain, because their preintegration complex enters the nuclei without mitosis (Naldini et al., 1996; Lever et al., 2004). In addition, there seems a consensus that lentivirus vectors gain advantages over adenoviral and adeno-associated viral vectors in terms of the stability and/or sensitivity. The present study provides evidence that HIV-1-based, but not SIV-based, lentiviral vectors possess the high tropism to neurons and permit retrograde transport of an expressed gene, especially in primates. If the latter property can be improved at a practical level, then the use of HIV-1-based lentiviral vectors may carry a potential benefit in the treatment of Parkinson's disease that is caused by degeneration of the nigrostriatal dopaminergic system. Stereotaxic injections of the vectors into the spatially larger target, the striatum, with greater certainty would avoid high risks of surgical damage and/or unnecessary diffusion to surrounding normal structures which might result from the injections into the SNc lying deep in the brain.

Acknowledgements

We thank Michiko Imanishi and Etsuko Mine for excellent technical assistance. This work was supported in part by

Grants-in-Aid from the Ministry of Education, Culture, Sports, Science and Technology of Japan.

References

Baekelandt, V., Claeys, A., Eggermont, K., Lauwers, E., De Strooper, B., Nuttin, B., Debyser, Z., 2002. Characterization of lentiviral vector-mediated gene transfer in adult mouse brain. Hum. Gene Ther. 13, 841–853.

Bensadoun, J.C., Déglon, N., Tseng, J.L., Ridet, J.L., Zurn, A.D., Aebischer, P., 2000. Lentiviral vectors as a gene delivery system in the mouse midbrain: cellular and behavioral improvements in a 6-OHDA model of Parkinson's disease using GDNF. Exp. Neurol. 164, 15–24.

Brizard, M., Carcenac, C., Bemelmans, A.P., Feuerstein, C., Mallet, J., Savasta, M., 2006. Functional reinnervation from remaining DA terminals induced by GDNF lentivirus in a rat model of early Parkinson's disease. Neurobiol. Dis. 21, 90–101.

Crystal, R.G., Sondhi, D., Hackett, N.R., Kaminsky, S.M., Worgall, S., Stieg, P., Souweidane, M., Hosain, S., Heier, L., Ballon, D., Dinner, M., Wisniewski, K., Kaplitt, M., Greenwald, B.M., Howell, J.D., Strybing, K., Dyke, J., Voss, H., 2004. Clinical protocol. Administration of a replication-deficient adeno-associated virus gene transfer vector expressing the human CLN2 cDNA to the brain of children with late infantile neuronal ceroid lipofuscinosis. Hum. Gene Ther. 15, 1131–1154.

Déglon, N., Tseng, J.L., Bensadoun, J.C., Zurn, A.D., Arsenijevic, Y., Pereira de Almeida, L., Zufferey, R., Trono, D., Aebischer, P., 2000. Self-inactivating lentiviral vectors with enhanced transgene expression as potential gene transfer system in Parkinson's disease. Hum. Gene Ther. 11, 179–190.

Dowd, E., Monville, C., Torres, E.M., Wong, L.F., Azzouz, M., Mazarakis, N.D., Dunnett, S.B., 2005. Lentivector-mediated delivery of GDNF protects complex motor functions relevant to human Parkinsonism in a rat lesion model. Eur. J. Neurosci. 22, 2587–2595.

Ferrarese, C., Sala, G., Riva, R., Begni, B., Zoia, C., Tremolizzo, L., Galimberti, G., Millul, A., Bastone, A., Mennini, T., Balzarini, C., Frattola, L., Beghi, E., 2001. Decreased platelet glutamate uptake in patients with amyotrophic lateral sclerosis. Neurology 56, 270–272.

Georgievska, B., Jakobsson, J., Persson, E., Ericson, C., Kirik, D., Lundberg, C., 2004. Regulated delivery of glial cell line-derived neurotrophic factor into rat striatum, using a tetracycline-dependent lentiviral vector. Hum. Gene Ther. 15, 934–944.

Hanawa, H., Hematti, P., Keyvanfar, K., Metzger, M.E., Krouse, A., Donahue, R.E., Kepes, S., Gray, J., Dunbar, C.E., Persons, D.A., Nienhuis, A.W., 2004. Efficient gene transfer into rhesus repopulating hematopoietic stem cells using a simian immunodeficiency virus-based lentiviral vector system. Blood 103, 4062–4069.

Janson, C., McPhee, S., Bilaniuk, L., Haselgrove, J., Testaiuti, M., Freese, A., Wang, D.J., Shera, D., Hurh, P., Rupin, J., Saslow, E., Goldfarb, O., Goldberg, M., Larijani, G., Sharrar, W., Liouterman, L., Camp, A., Kolodny, E., Samulski, J., Leone, P., 2002. Clinical protocol. Gene therapy of Canavan disease: AAV-2 vector for neurosurgical delivery of aspartoacylase gene (ASPA) to the human brain. Hum. Gene Ther. 13, 1391–1412.

Kordower, J.H., Bloch, J., Ma, S.Y., Chu, Y., Palfi, S., Roitberg, B.Z., Emborg, M., Hantraye, P., Déglon, N., Aebischer, P., 1999. Lentiviral gene transfer to the nonhuman primate brain. Exp. Neurol. 160, 1–16.

Kordower, J.H., Emborg, M.E., Bloch, J., Ma, S.Y., Chu, Y., Leventhal, L., McBride, J., Chen, E.Y., Palfi, S., Roitberg, B.Z., Brown, W.D., Holden, J.E., Pyzalski, R., Taylor, M.D., Carvey, P., Ling, Z., Trono, D., Hantraye, P., Déglon, N., Aebischer, P., 2000. Neurodegeneration prevented by lentiviral vector delivery of GDNF in primate models of Parkinson's disease. Science 290, 767–773.

Kyrkanides, S., Miller, J.H., Brouxhon, S.M., Olschowka, J.A., Federoff, H.J., 2005. beta-hexosaminidase lentiviral vectors: transfer into the CNS via systemic administration. Mol. Brain Res. 133, 286–298.

Lai, Z., Brady, R.O., 2002. Gene transfer into the central nervous system *in vivo* using a recombinanat lentivirus vector. J. Neurosci. Res. 67, 363–371.

Lever, A.M., Strappe, P.M., Zhao, J., 2004. Lentiviral vectors. J. Biomed. Sci. 11, 439–449.

Lo Bianco, C., Schneider, B.L., Bauer, M., Sajadi, A., Brice, A., Iwatsubo, T., Aebischer, P., 2004. Lentiviral vector delivery of parkin prevents dopaminergic degeneration in an alpha-synuclein rat model of Parkinson's disease. Proc. Natl. Acad. Sci. U.S.A. 101, 17510–17515.

Marr, R.A., Rockenstein, E., Mukherjee, A., Kindy, M.S., Hersh, L.B., Gage, F.H., Verma, I.M., Masliah, E., 2003. Neprilysin gene transfer reduces human amyloid pathology in transgenic mice. J. Neurosci. 23, 1992–1996.

Mochizuki, H., Schwartz, J.P., Tanaka, K., Brady, R.O., Reiser, J., 1998. High-titer human immunodeficiency virus type 1-based vector systems for gene delivery into nondividing cells. J. Virol. 72, 8873–8883.

Nakao, N., Shintani-Mizushima, A., Kakishita, K., Itakura, T., 2004. The ability of grafted human sympathetic neurons to synthesize and store dopamine: a potential mechanism for the clinical effect of sympathetic neuron autografts in patients with Parkinson's disease. Exp. Neurol. 188, 65–73.

Naldini, L., Blomer, U., Gage, F.H., Trono, D., Verma, I.M., 1996. Efficient transfer, integration, and sustained long-term expression of the transgene in adult rat brains injected with a lentiviral vector. Proc. Natl. Acad. Sci. U.S.A. 93, 11382–11388.

Nègre, D., Cosset, F.-L., 2002. Vectors derived from simian immunodeficiency virus (SIV). Biochimie 84, 1161–1171.

Popovic, N., Maingay, M., Kirik, D., Brundin, P., 2005. Lentiviral gene delivery of GDNF into the striatum of R6/2 Huntington mice fails to attenuate behavioral and neuropathological changes. Exp. Neurol. 193, 65–74.

Rosenblad, C., Georgievska, B., Kirik, D., 2003. Long-term striatal over-expression of GDNF selectively downregulates tyrosine hydroxylase in the intact nigrostriatal dopamine system. Eur. J. Neurosci. 17, 260–270.

Sajadi, A., Bauer, M., Thony, B., Aebischer, P., 2005. Long-term glial cell line-derived neurotrophic factor overexpression in the intact nigrostriatal system in rats leads to a decrease of dopamine and increase of tetrahydrobiopterin production. J. Neurochem. 93, 1482–1486.

Scherr, M., Battmer, K., Eder, M., Schule, S., Hohenberg, H., Ganser, A., Grez, M., Blomer, U., 2002. Efficient gene transfer into the CNS by lentiviral vectors purified by anion exchange chromatography. Gene Ther. 9, 1708–1714.

Song, B., Javanbakht, H., Perron, M., Park, D.H., Stremlau, M., Sodroski, J., 2005. Retrovirus restriction by TRIM5alpha variants from Old World and New World primates. J. Virol. 79, 3930–3937.

Stedman, H., Wilson, J.M., Finke, R., Kleckner, A.L., Mendell, J., 2000. Phase I clinical trial utilizing gene therapy for limb girdle muscular dystrophy: alpha-, beta-, gamma-, or delta-sarcoglycan gene delivered with intramuscular instillations of adeno-associated vectors. Hum. Gene Ther. 11, 777–790.

Stremlau, M., Owens, C.M., Perron, M.J., Kiessling, M., Autissier, P., Sodroski, J., 2004. The cytoplasmic body component TRIM5alpha restricts HIV-1 infection in Old World monkeys. Nature 427, 848–853.

Tuszynski, M.H., Thal, L., Pay, M., Salmon, D.P., U, H.S., Bakay, R., Patel, P., Blesch, A., Vahlsing, H.L., Ho, G., Tong, G., Potkin, S.G., Fallon, J., Hanson, L., Mufson, E.J., Kordower, J.H., Gall, C., Conner, J., 2005. A phase 1 clinical trail of nerve growth factor gene therapy for Alzheimer disease. Nat. Med. 11, 551–555.

Volsky, B., Sakai, K., Reddy, M.M., Volsky, D.J., 1992. A system for the high efficiency replication of HIV-1 in neural cells and its application to antiviral evaluation. Virology 186, 303–308.

Wong, L.F., Ralph, G.S., Walmsley, L.E., Bienemann, A.S., Parham, S., Kingsman, S.M., Uney, J.B., Mazarakis, N.D., 2005. Lentiviral-mediated delivery of Bcl-2 or GDNF protects against excitotoxicity in the rat hippocampus. Mol. Ther. 11, 89–95.

Clinical Immunology (2006) 119, 188–194

available at www.sciencedirect.com

SCIENCE DIRECT®

www.elsevier.com/locate/yclim

A missense mutation of the Toll-like receptor 3 gene in a patient with influenza-associated encephalopathy

Fumio Hidaka [a], Susumu Matsuo [b], Tatsushi Muta [b], Koichiro Takeshige [b], Tomoyuki Mizukami [a], Hiroyuki Nunoi [a,*]

[a] *Department of Pediatrics, Miyazaki Medical College, University of Miyazaki, 5200 Kihara, Kiyotake-Chou, Miyazaki-Gun, Miyazaki 889-1692, Japan*

[b] *Department of Molecular and Cellular Biochemistry, Graduate School of Medical Sciences, Kyushu University, 3-1-1, Maidashi, Higashi-ku, Fukuoka 812-8582, Japan*

Received 9 August 2005; accepted with revision 17 January 2006
Available online 6 March 2006

KEYWORDS
Toll-like receptor;
Innate immunity;
RNA virus;
Influenza-associated encephalopathy;
Missense mutation

Abstract Toll-like receptors (TLRs) recognize pathogen-associated molecular patterns and mediate the activation of NF-κB and the production of proinflammatory cytokines, which is critical for the innate immune system. TLR3 recognizes both double-stranded RNA and the influenza A virus. Since influenza-associated encephalopathy is frequent in Japan and East Asia and its pathological mechanism remains unknown, we analyzed several genes including TLRs and the retinoic acid inducible gene I, which could be involved in the recognition of the RNA virus. In one of three patients with influenza-associated encephalopathy, we detected a novel missense mutation (F303S) in just the *TLR3* gene. This was confirmed as a loss-of-function mutant in a dose-dependent manner by NF-κB and IFN-β reporter assays using wild-type and mutant TLR3-transfected HEK293 cells. Our results imply that a mutation of the *TLR3* gene could be one of the factors responsible for influenza-associated encephalopathy.

Introduction

Toll-like receptors (TLRs) are type I transmembrane proteins with an extracellular domain consisting of a leucine-rich repeat (LRR) domain, and a cytoplasmic Toll/IL-1 receptor homology (TIR)-domain [1]. TLRs activate NF-κB to produce inflammatory cytokines through common signaling molecules; myeloid differentiation factor 88 (MyD88), IL-1 RI-associated protein kinases, and the tumor necrosis factor receptor-associated factor 6 (TRAF6) [2].

Ten members of the TLR family have been identified in human [3–6]. TLR1, 2, 4, 5, and 6 interact with bacterial pathogen-associated molecular patterns (PAMPs) such as peptidoglycan, lipopolysaccharide, lipoprotein, and flagellin [7–10], whereas ligands of TLRs2 and 4 have also been

* Corresponding author. Fax: +81 985 85 2403.
E-mail address: h-nunoi@fc.miyazaki-u.ac.jp (H. Nunoi).

1521-6616/$ – see front matter © 2006 Elsevier Inc. All rights reserved.
doi:10.1016/j.clim.2006.01.005

identified to include viral particles [11–13]. A polymorphism in the *TLR2* gene has been identified to predispose to staphylococcal infection [14]; whereas mutations in the *TLR4* gene are responsible for endotoxin hyporesponsiveness, gram-negative septic shock, and ulcerative colitis [15–17]; and those in the *nucleotide-binding oligomerization domain (NOD)-2* gene for Crohn's disease and Blau syndrome [18–20]. TLRs3 and 7/8 recognize nucleotide derivatives; double-stranded RNA (dsRNA) and single-stranded RNA (ssRNA), respectively [21–24]. TLR3 was found to contribute directly to the immune response of respiratory epithelial cells to dsRNA and the influenza A virus [25].

The *TLR3* gene is mapped to chromosome 4q35 [3], and its open reading frame encoded by four exons. Its mRNA is 3029 base pairs in length and is detected in many organs [3,26]. In leukocytes, it is expressed in dendritic cells (DCs) but not in monocytes, lymphocytes, polymorphonuclear leukocytes, or natural killer cells [27]. In immature DCs, TLR3 is expressed intracellularly [28], whereas in human fibroblasts and epithelial cells, it is expressed both on the cell surface and inside cells [29]. TLR3 consists of 904 amino acids with an extracellular domain of 23 LRRs, a transmembrane region, and a TIR domain [30]. TLR3 activates NF-κB and interferon regulatory factor (IRF)-3 independently of MyD88 through a TIR domain-containing adapter inducing IFN-β [21,31].

Children suffering from an influenza infection can exhibit complications including typical febrile convulsion, decreased sensorium, delirium, and finally a deep, irreversible coma. Influenza-associated encephalopathy is reported to be more frequent in East Asia than in the west [32–34]. In Japan, the total number of fatal cases of influenza-associated encephalopathy was estimated at 100–200 per season [35] (22.65 deaths per 100,000 persons [36]).

Since influenza-associated encephalopathy develops within the first few days after infection, we considered that innate, but not acquired immunity could be associated with influenza-associated encephalopathy. Based on several pro-inflammatory cytokines and cytochrome *c* assays, we concluded that apoptosis of tissue under hypercytokinemia could be a cause of influenza-associated encephalopathy [37]. Recently, expression of TLRs and their mediators were found to be increased by influenza A virus infection [38]. However, the mechanism of hypercytokinemia remains unclear.

In this study of three patients with influenza-associated encephalopathy, we analyzed some members of the TLR family and the retinoic acid inducible gene I (RIG-I), all of which could be involved in the recognition of RNA viruses, and found a missense mutation of the *TLR3* gene in one patient. We propose that the *TLR3* mutation could be associated with severe influenza complications.

Patients, materials, and methods

Patients

Three patients were given a diagnosis of influenza-associated encephalopathy on the basis of their clinical courses, computed tomography (CT), magnetic resonance imaging findings, and a viral antigen test, Espline Influenza A&B-N (Fujirebio Inc., Tokyo, Japan). With informed consent, the *TLRs3*, *7*, *8*, and *RIG-I* genes were analyzed. We describe below the patient in whom we detected a missense mutation of the *TLR3* gene.

The patient was a 4-year-old Japanese girl who had developed normally under a prescription of levothyroxine sodium (30 μg/day) due to hypothyroidism. She visited our hospital complaining of high fever (>39°C) and a cough that she had since the night before. A viral antigen test indicated a diagnosis of influenza A virus infection, and so oseltamivir was prescribed. Two hours later, she suffered convulsions and loss of consciousness, followed by vomiting. She was treated with diazepam (20 mg) intravenously but remained in a convulsive state, and showed decreased sensorium and shallow breathing. She was intubated and given a diagnosis of influenza-associated encephalopathy on the basis of brain edema detected by CT. Subsequently, a high dose of intravenous gamma globulin (1 g/kg) was administered for 1 day, methylpredonisolone (30 mg/kg) for 3 days, and a depressor of intracranial pressure, mannitol (5 mg/kg × 6), for 5 days. Her body temperature was kept at 34°C (systemic hypothermia therapy) to prevent hypercytokinemia and secondary brain damage, according to our experiences and guidelines issued for influenza-associated encephalopathy in Japan [39].

Laboratory data on admission showed normal hepatic and renal functions and coagulation status (TP 6.04 g/dl, AST 29 IU/L, ALT 14 IU/L, LDH 243 IU/L, NH_3 52 μg/dl, T-bil 0.4 mg/dl, BUN 10.8 mg/dl, Cre 0.4 mg/dl, ATIII 90%, plasminogen 68%, fibrinogen 206 mg/dl, D-dimer 1.76 μg/ml, prothrombin time 14.2 s) but a subnormal electrolytic status (Na 128 mEq/L, K 3.3 mEq/L, Cl 99 mEq/L) and elevated CRP (2.2 mg/dl).

Since an improvement of the brain edema was confirmed on the fifth day after admission, her body temperature was returned stepwise to a normal temperature (0.5°C/day). On the 11th day, she was extubated and could speak a few words. On the 13th day, she was transferred from the intensive care unit to the pediatric division. Subsequently, she was discharged with neurological sequelae; restlessness and hyperactivity, which lasted for a year. Single photon emission CT showed decreased perfusion in the right frontal, temporal, and occipital lobes, which improved eight months after discharge.

Genetic analysis

Genomic DNA was extracted from whole blood by Puregene DNA isolation kit (Gentra Systems, Minneapolis, MN). Nine pairs of polymerase chain reaction (PCR) primers were constructed to encompass the open reading frame of the *TLR3* gene (Table 1). PCR primers were also constructed to amplify the *TLRs7*, *8*, and *RIG-I* genes in accord with a previous report [5] and the database of GenBank in the National Center for Biotechnology Information (NCBI). The reaction mixture (25 μL) contained 10 mM Tris–HCL, pH 8.3, 50 mM KCl, 1.5 mM $MgCl_2$, each dNTP and Ampli Taq Gold (ABI, Foster City, CA). PCR for the *TLR3* gene was performed under the following conditions; the first denaturation at 95°C for 9 min was followed by 45 cycles of denaturation at 95°C for 1 min, annealing at 58°C for 1 min, and extension at 72°C for 1 min. The final extension was performed at 72°C for 7 min. PCR products were sequenced directly with an ABI PRISM BigDye Terminator Cycle Sequencing FS Ready

Table 1 PCR primers of the TLR3 gene

	Forward primer	Reverse primer	Amplified region
A-1	GAGTAATAACATCATACATGG	CTGGCACAATTCTGGCTC	1–350
A-2	GGTATAGCCAGCTAACTAGC	GTCTAAGGATGGGTATCTG	351–514
B-1	GTATTCTACAGAATAATAGAG	GATTGCTGGAAGACAGGCAG	515–706
C-1	CAGCATTACAGAGTCTGTG	CATCAATCTTGGGGAGTGAG	707–1100
C-2	GTGAGGTACCTGAATTTG	GAGCATCAGTCGTTGAAGGC	1100–1520
C-3	GTACCTGCAGCTGACTAGG	CTTCTCAACGGATGTTATG	1521–1940
C-4	GGTGTCTCTAAAGTCATTG	GCATATTCAAACTGTTCTGTC	1941–2330
C-5	CAGTACATCGAGTTCTTGG	CACTTAAAATTTCACAATG	2331–2559
D-1	CCTGAGTTTCAGTAACAG	CCTAGAAGAGATGTAATTGTG	2560–2788

Reaction Kit (ABI). Sequencing was performed with an ABI model 310.

Luciferase reporter assay

HEK293 cells (3×10^5 cells) were transfected with expression plasmids (450 ng) and the NF-κB reporter plasmid [40] (pELAM-1-Luc, 150 ng) or an IFN-β reporter plasmid [41] (150 ng) together with the internal control plasmid phRL-TK-Luc (Promega Corp., Madison, WI, 15 ng) by the calcium phosphate precipitation method [42]. Eighteen hours after transfection, the cells were stimulated with 10 μg/ml poly (I:C) (Sigma, St. Louis, MO) for 6 h. The stimulated cells were lysed and luciferase activity was measured by a Dual Luciferase™ reporter assay system (Promega Corp.) according to the manufacturer's instructions. The activity of the reporter was normalized on the basis of *Renilla* luciferase activity. Data shown are the mean ± SEM of duplicate samples and are representative of at least two independent experiments. In this study, both pcDNA (Invitrogen Corp., Carlsbad, CA) and pFLAG-CMV (Promega Corp.) were employed for functional assay.

Western blotting

HEK293 cells were transfected as in the luciferase reporter assay. Twenty-four hours after transfection, cell lysate was prepared and subjected to Western blotting analysis with anti-FLAG M2 monoclonal antibody–peroxidase conjugate (Sigma). Reacting proteins were visualized by chemiluminescence using Lumi-Light^{Plus} Western blotting substrate (Roche Diagnostics, Indianapolis, IN).

Results

Genetic analysis and reporter assays

We performed genetic analyses in the three patients with influenza-associated encephalopathy and identified a missense mutation of the *TLR3* gene in one, in whom no

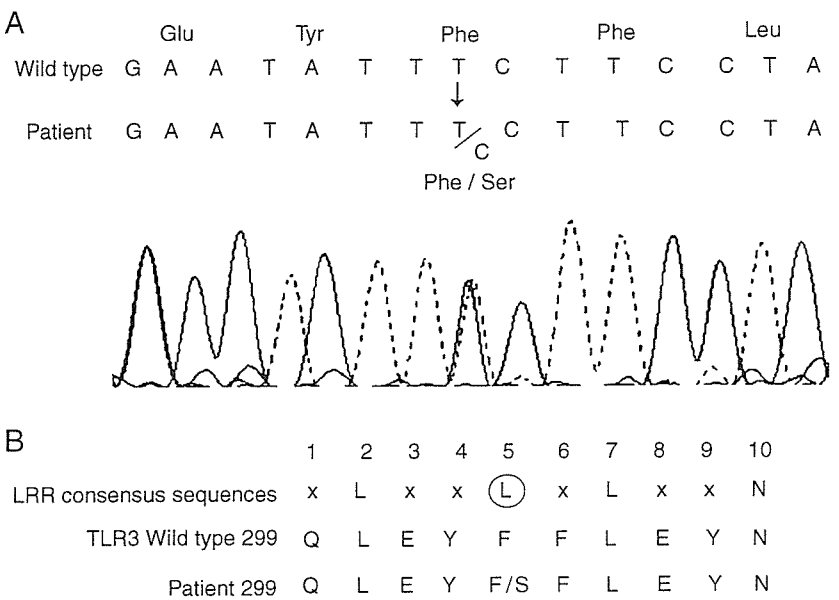

Figure 1 Genetic analysis of the *TLR3* gene. The patient's *TLR3* coding sequences were analyzed by direct sequencing. A single substitution of T (broken line) to C (solid gray line) at nucleotide position 908 causes the replacement of phenylalanine with serine at amino acid position 303 (A). LRR consensus sequences and the 11th LRR of TLR3 are shown (B). The Phenylalanine at position 303 (circle) is conserved in the LRR motif of TLR and other LRR-containing proteins. x refers to any amino acid. L is frequently replaced by other hydrophobic residues.

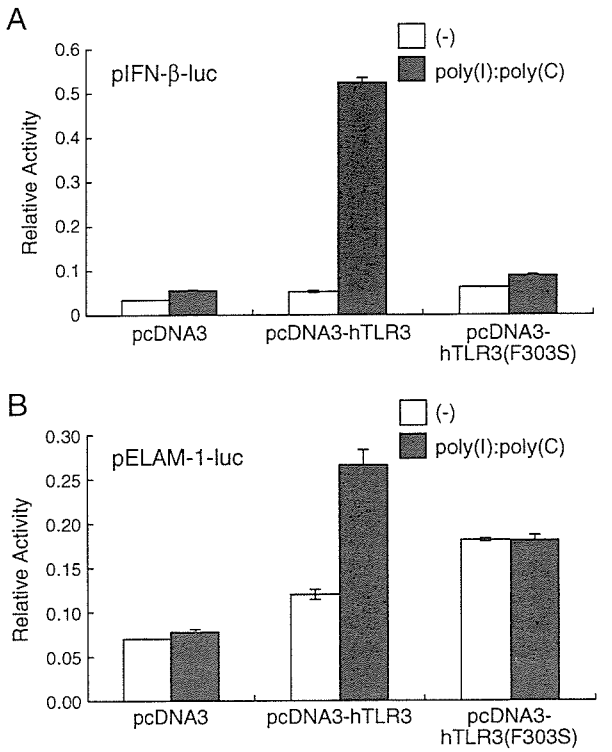

Figure 2 IFN-β and NF-κB reporter assays. HEK 293 cells (3×10^5 cells) were co-transfected with 450 ng of indicated expression plasmids and 150 ng of pIFN-β-luc (A) or pELAM-1-luc (B) reporter plasmid together with phRL-TK-luc. Eighteen hours after transfection, cells were stimulated with medium with or without 10 μg/ml poly(I:C) for 6 h, and luciferase activities were measured.

mutations were found in the *TLRs7*, *8*, and *RIG-I* genes. A single substitution of T to C at nucleotide position 908 of the *TLR3* gene was confirmed, which caused an amino acid transition of phenylalanine to serine at position 303 (Fig. 1A). The patient was heterozygous for the mutation, which was located in the 11th of 23 LRRs in the *TLR3* gene. We found no mutations in the *TLRs3*, *7*, *8*, or *RIG-I* genes in the other patients.

IFN-β and NF-κB reporter assays were employed to evaluate the function of the mutant TLR3(F303S). HEK293 cells were transfected with expression plasmids for human TLR3 (wild type or mutant) together with luciferase-reporter plasmids. Stimulation with poly(I:C) induced the activation of IFN-β promoter activity in the TLR3-transfected cells, but not in the mutant-transfected cells (Fig. 2A). NF-κB activity was elevated in the TLR3-transfected cells, while NF-κB activity was not induced with or without stimulation of poly(I:C) in the mutant-transfected cells (Fig. 2B). To confirm whether the mutant TLR3(F303S) could inhibit IFN-β promoter and NF-κB activities depending on its amount in a dominant-negative way or a dose-dependent way, the cells were co-transfected with 225 ng of negative control expression plasmids, pcDNA3 (Fig. 3A), or the mutant plasmid, pcDNA3 hTLR3 (F303S) (Fig. 3B), and 0, 14, 28, 56, 113, and 225 ng of the human TLR3. IFN-β promoter activities elevated in a dose-dependent manner in cells co-transfected with negative control and the wild type (Fig. 3A) but seemed to be depressed in cells co-transfected with the mutant and the wild type (Fig. 3B) compared with former ones. To ascertain a dominant-negative effect, the cells were co-transfected with fixed amounts of the human TLR3 and the various concentrations of the mutant. These studies confirmed that dominant-negative effect is unlikely (Fig. 4). Western blotting was performed to confirm the

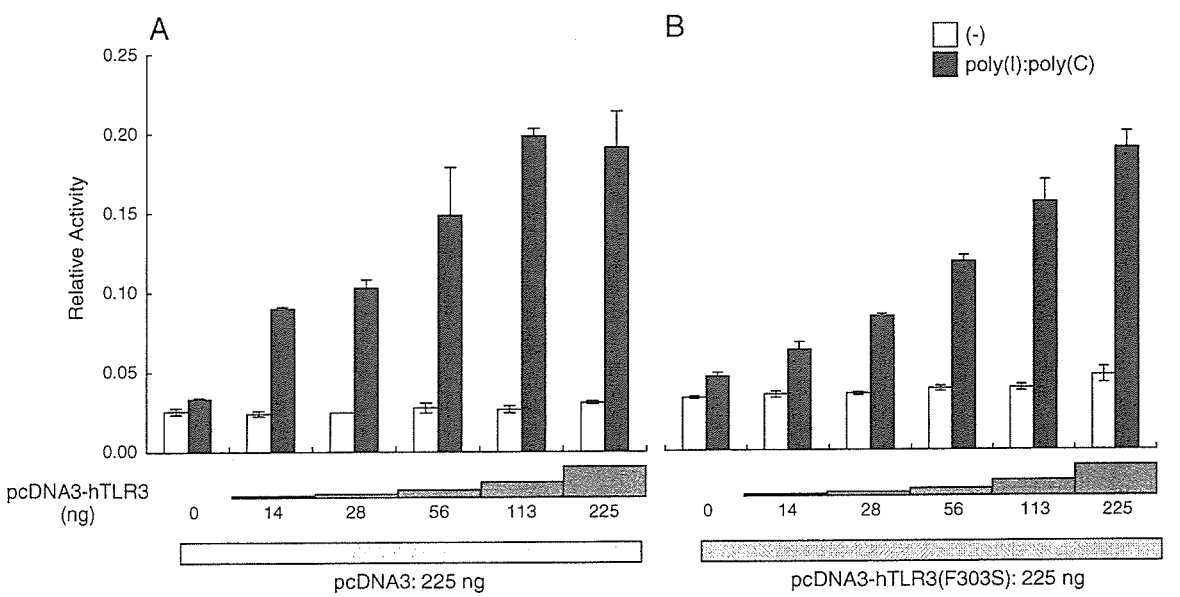

Figure 3 Co-transfection of TLR3 and TLR3(F303S). HEK 293 cells were co-transfected with indicated amounts of expression plasmids and 150 ng of the reporter plasmid, pIFN-β-luc, together with phRL-TK-luc. The total amount of DNA was kept constant with an empty vector (total 600 ng).

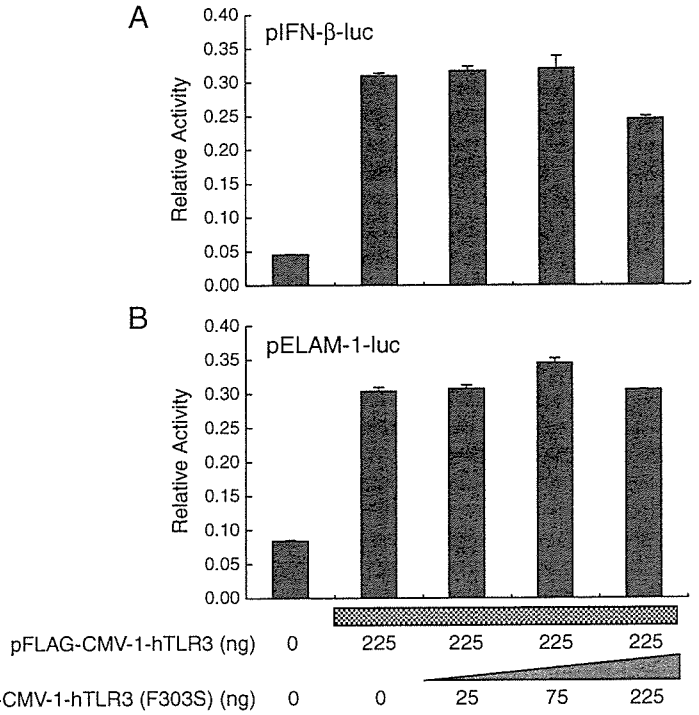

Figure 4 Co-transfection with TLR3(F303S) and fixed amounts of TLR3. HEK 293 cells were co-transfected with indicated amounts of expression plasmids together with the reporter plasmid, pIFN-β-luc (A) or pELAM-1-luc (B), and phRL-TK-luc. The total amount of DNA was kept constant with an empty vector. Eighteen hours after transfection, cells were stimulated with the medium with or without 10 μg/ml poly(I:C) for 6 h, and luciferase activities were measured.

expression levels of TLR3 and the mutant transfected with FLAG-tagged expression plasmids. The mutant was expressed at levels comparable to those of the wild type (Fig. 5). Expression levels were also monitored and normalized in all experiments by *Reralla* luciferase activity co-transfected with the internal control plasmid phRL-Tk-Luc.

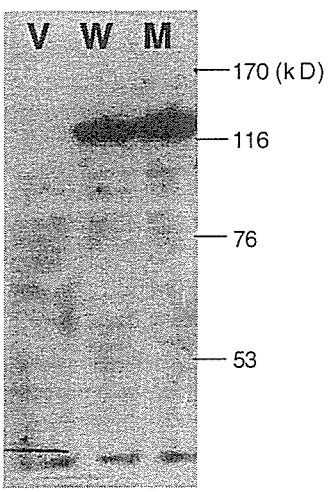

Figure 5 Western blotting. HEK 293 cells (3×10^5 cells) were transfected with 450 ng of indicated expression plasmids pcDNA3(V), pFLAG-CMV-1-hTLR3(W), or pFLAG-CMV-1-hTLR3(F303S)(M). Twenty-four hours after transfection, cell extracts were prepared. Immunoblotting analysis was performed with anti-FLAG antibody (SIGMA M2).

Discussion

One of the three patients with influenza-associated encephalopathy in our study had a novel missense mutation of the *TLR3* gene. A single substitution of T to C at nucleotide position 908, which caused an amino acid transition of hydrophobic phenylalanine to hydrophilic serine at position 303 (Fig. 1A), likely changes its conformation in the LRR domain. As the hydrophobic amino acid (leucine or phenylalanine) in the 11th LRR is conserved in TLRs and other LRR-containing proteins [30] (Fig. 1B), we suspect that phenylalanine in the 11th LRR is functionally important to the LRR domain of TLR3. We speculate that the structure of LRR might be impaired in its recognition of RNA viruses in mutant TLR3. Although seven single nucleotide polymorphisms of the *TLR3* gene have been reported in the NCBI databases, mutations at nucleotide position 908 had not previously been reported. No mutations at the same position were found in our 20 healthy controls.

By transfection assay with expression plasmids of wild-type and mutant TLR3 in HEK293 cells, IFN-β promoter and NF-κB activities were detected in the wild type but not in the mutant after stimulation with poly (I:C) (Fig. 2). These results suggest that mutant TLR3 is a loss-of-function mutation. Subsequently, IFN-β promoter and NF-κB activities were measured by a co-transfection assay with wild-type and mutant TLR3 in HEK293 cells. Although the mutant TLR3 was expressed at levels comparable to those of the wild type in HEK293 cells (Fig. 5), IFN-β promoter activities were seen to elevate in a dose-dependent manner (Fig. 3). These results suggest that the mutant TLR3 may have a dose

effect but was unlikely to have a dominant-negative effect in this assay system for intracellular signaling.

As with our TLR3 studies in vitro, Alexopoulou et al. [21] reported using TLR3−/− mice that macrophages and splenocytes showed a reduced, but not completely inhibited, response in inflammatory cytokine production after poly(I:C) stimulation. However, NF-κB activation under hypercytokinemia conditions is often detected in patients with influenza-associated encephalopathy [37,43]. Such controversial results in vitro and in vivo studies have been reported in the TLR-related protein NOD2. Transient transfection experiments using HEK293 cells characterized the mutant 3020 insC as having a loss-of-function [44], whereas knock-in mouse studies showed macrophages with the same mutant NOD2 as having a gain-of-function [45].

We consider that heterozygous expression of the mutant and wild-type TLR3 may have a dose-dependent effect, being reduced to a level half of TLR3 activating signals, comparing to the full expression of the wild-type TLR3. Consequently, a reduced response by heterozygous TLR3 might allow transient excess proliferations of invading influenza viruses, and secondary responses through other pathways (other TLRs, their mediators, and RIG-I etc.) are likely to enhance higher cytokine production.

Although further studies will be needed to clarify the association of a *TLR3* mutation and influenza-associated encephalopathy, we report the first case of influenza-associated encephalopathy with a novel missense mutation of the *TLR3* gene, which we characterized as a loss-of-function mutant in HEK293 cells.

Acknowledgments

We are grateful to the patient and her family for participating in this study. We thank Drs. H. Sawada and M. Matsuyama (Miyazaki Medical College) for providing us with useful information related to this patient.

Appendix A. Supplementary data

Supplementary data associated with this article can be found in the online version at doi:10.1016/j.clim.2006.01.005.

References

[1] R. Medzhitov, P. Preston-Hurlburt, C.A. Janeway Jr., A human homologue of the *Drosophila* Toll protein signals activation of adaptive immunity, Nature 388 (1997) 394-397.
[2] S. Akira, Toll-like receptor signaling, J. Biol. Chem. 278 (2003) 38105-38108.
[3] F.L. Rock, G. Hardman, J.C. Timans, R.A. Kastelein, J.F. Bazan, A family of human receptors structurally related to *Drosophila* Toll, Proc. Natl. Acad. Sci. U. S. A. 95 (1998) 588-593.
[4] O. Takeuchi, T. Kawai, H. Sanjo, et al., TLR6: a novel member of an expanding toll-like receptor family, Gene 231 (1999) 59-65.
[5] X. Du, A. Poltorak, Y. Wei, B. Beutler, Three novel mammalian toll-like receptors: gene structure, expression, and evolution, Eur. Cytokine Netw. 11 (2000) 362-371.
[6] T.H. Chuang, R.J. Ulevitch, Identification of hTLR10: a novel human Toll-like receptor preferentially expressed in immune cells, Biochem. Biophys. Acta 1518 (2001) 157-161.
[7] A. Aderem, R.J. Ulevitch, Toll-like receptors in the induction of the innate immune response, Nature 406 (2000) 782-787.
[8] A. Ozinsky, D.M. Underhill, J.D. Fontenot, et al., The repertoire for pattern recognition of pathogens by the innate immune system is defined by cooperation between Toll-like receptors, Proc. Natl. Acad. Sci. U. S. A. 97 (2000) 13766-13771.
[9] F. Hayashi, K.D. Smith, A. Ozinsky, et al., The innate immune response to bacterial flagellin is mediated by Toll-like receptor 5, Nature 410 (2001) 1099-1103.
[10] O. Takeuchi, S. Sato, T. Horiuchi, et al., Cutting edge: role of Toll-like receptor 1 in mediating immune response to microbial lipoproteins, J. Immunol. 169 (2002) 10-14.
[11] L.M. Haynes, D.D. Moore, E.A. Kurt-Jones, R.W. Finberg, L.J. Anderson, R.A Tripp, Involvement of Toll-like receptor 4 in innate immunity to respiratory syncytial virus, J. Virol. 75 (2001) 10730-10737.
[12] K. Bieback, E. Lien, I.M. Klagge, et al., Hemagglutinin protein of wild-type measles virus activates Toll-like receptor 2 signaling, J. Virol. 76 (2002) 8729-8736.
[13] T. Compton, E.A. Kurt-Jones, K.W. Boehme, et al., Human cytomegalovirus activates inflammatory cytokine responses via CD14 and Toll-like receptor 2, J. Virol. 77 (2003) 4588-4596.
[14] E. Lorenz, J.P. Mira, K.L. Cornish, N.C. Arbour, D.A. Schwartz, A novel polymorphism in the Toll-like receptor 2 gene and its potential association with staphylococcal infection, Infect. Immun. 68 (2000) 6398-6401.
[15] N.C. Arbour, E. Lorenz, B.C. Schutte, et al., TLR4 mutations are associated with endotoxin hyporesponsiveness in humans, Nat. Genet. 25 (2000) 187-191.
[16] E. Lorenz, J.P. Mira, K.L. Frees, D.A. Schwartz, Relevance of mutations in the TLR4 receptor in patients with gram-negative septic shock, Arch. Intern. Med. 162 (2002) 1028-1032.
[17] H.P. Torok, J. Glas, L. Tonenchi, T. Mussack, C. Flowaczny, Polymorphisms of the lipopolysaccharide-signaling complex in inflammatory bowel disease: association of a mutation in the Toll-like receptor 4 gene with ulcerative colitis, Clin. Immunol. 112 (2004) 85-91.
[18] J.P. Hugot, M. Chamaillard, H. Zouali, et al., Association of NOD2 leucine-rich repeat variants with susceptibility to Crohn's disease, Nature 411 (2001) 599-603.
[19] Y. Ogura, D.K. Bonen, N. Inohara, et al., A frameshift mutation in NOD2 associated with susceptibility to Crohn's disease, Nature 411 (2001) 603-606.
[20] C. Miceli-Richard, S. Lesage, M. Rybojad, et al., CARD15 mutations in Blau syndrome, Nat. Genet. 29 (2001) 19-20.
[21] L. Alexopoulou, A.C. Holt, R. Medzhitov, R.A. Flavell, Recognition of double-stranded RNA and activation of NF-κB by Toll-like receptor 3, Nature 413 (2001) 732-738.
[22] F. Heil, H. Hemmi, H. Hochrein, et al., Species-specific recognition of single stranded RNA via Toll-like receptor 7 and 8, Science 303 (2004) 1526-1529.
[23] S.S. Diebold, T. Kaisho, H. Hemmi, S. Akira, C. Reis e Sousa, Innate antiviral responses by means of TLR7-mediated recognition of single-stranded RNA, Science 303 (2004) 1529-1531.
[24] K. Crozat, B. Beutler, TLR7: a new sensor of viral infection, Proc. Natl. Acad. Sci. U. S. A. 101 (2004) 6835-6836.
[25] L. Guillot, R.L. Goffic, S. Bloch, et al., Involvement of Toll-like receptor 3 in the immune response of lung epithelial cells to double-stranded RNA and influenza A virus, J. Biol. Chem. 280 (2005) 5571-5580.
[26] E. Cario, D.K. Podolsky, Differential alteration in intestinal epithelial cell expression of Toll-like receptor 3 (TLR3) and TLR4 in inflammatory bowel disease, Infect. Immune. 68 (2000) 7010-7017.
[27] M. Muzio, D. Bosisio, N. Polentarutti, et al., Differential expression and regulation of Toll-like receptors (TLR) in human leukocytes: selective expression of TLR3 in dendritic cells, J. Immunol. 164 (2000) 5998-6004.